

## REVIEW ARTICLE OPEN



# On the future zonal contrasts of equatorial Pacific climate: Perspectives from Observations, Simulations, and Theories

Sukyong Lee<sup>1</sup>✉, Michelle L'Heureux<sup>2</sup>, Andrew T. Wittenberg<sup>3</sup>, Richard Seager<sup>4</sup>, Paul A. O'Gorman<sup>5</sup> and Nathaniel C. Johnson<sup>3</sup>

Changes in the zonal gradients of sea surface temperature (SST) across the equatorial Pacific have major consequences for global climate. Therefore, accurate future projections of these tropical Pacific gradients are of paramount importance for climate mitigation and adaptation. Yet there is evidence of a dichotomy between observed historical gradient trends and those simulated by climate models. Observational records appear to show a “La Niña-like” strengthening of the zonal SST gradient over the past century, whereas most climate model simulations project “El Niño-like” changes toward a weaker gradient. Here, studies of these equatorial Pacific climate trends are reviewed, focusing first on data analyses and climate model simulations, then on theories that favor either enhanced or weakened zonal SST gradients, and then on notable consequences of the SST gradient trends. We conclude that the present divergence between the historical model simulations and the observed trends likely either reflects an error in the model's forced response, or an underestimate of the multi-decadal internal variability by the models. A better understanding of the fundamental mechanisms of both forced response and natural variability is needed to reduce the uncertainty. Finally, we offer recommendations for future research directions and decision-making for climate risk mitigation.

*npj Climate and Atmospheric Science* (2022)5:82; <https://doi.org/10.1038/s41612-022-00301-2>

## INTRODUCTION

Future sea surface temperature (SST) changes in the equatorial Pacific will have major consequences for the global climate, mainly via their influence on deep convection in the tropical atmosphere. This deep convection tends to form where the SST is particularly high relative to the rest of the tropics, which is why the Indo-West Pacific warm pool is home to most of the world's atmospheric deep convection. The condensation of moisture within areas of deep convection releases latent heat, which drives or modulates much of the large-scale circulation of the tropical atmosphere (including the Hadley and Walker cells), and influences the extratropical circulation as far away as the Arctic and Antarctic. Tropical SST and convection patterns also affect tropical cyclone formation and development, the orientation of the extratropical Pacific storm track, and the risks of severe weather, floods, and droughts over the continents. The tropical Pacific is also the main oceanic source of CO<sub>2</sub> flux to the atmosphere. Tropical Pacific variability directly modulates the air-sea CO<sub>2</sub> flux and drives hydrological variability that also strongly influences continental vegetation, which serves as the main terrestrial sink of atmospheric CO<sub>2</sub>.

Most climate model simulations generally show similar *global mean* warming trends as those observed over the past century. Yet in the tropical Pacific region, observed multidecadal trends in large-scale SST, sea level pressure (SLP), and wind patterns have not been reproduced in most climate model simulations. Observational records appear to show strengthening zonal gradients in equatorial Pacific SST over the past century (Fig. 1A). SLP observations are more limited and uncertain prior to the 1950s, but afterward, the trend toward a weaker SLP zonal gradient slows, and then reverses toward a stronger gradient. A

tropical Pacific trend toward stronger SST and SLP zonal gradients may be described as roughly “La Niña-like,” even though the pattern and underlying physical mechanisms differ to some extent from La Niña, the cool phase of the naturally occurring seasonal-to-interannual climate mode known as the El Niño-Southern Oscillation (ENSO). (“El Niño-like” is used as a similar shorthand to describe trends toward weaker equatorial Pacific zonal gradients of SST and SLP, although again, the physical processes of the long-term El Niño-like model projections differ to some extent from those of seasonal-to-interannual El Niño events.) In contrast, most climate model simulations over the same period show a relative El Niño-like change toward weaker gradients, superimposed on tropics-wide warming (Fig. 1B). This El Niño-like trend becomes more pronounced in model projections of the 21st century, and the discrepancy between modeled and observed trends persists in the latest CMIP6 model simulations<sup>1,2</sup>. Future projections from these models are often used to plan climate mitigation and adaptation at regional scales, which will depend on the future state of the tropical Pacific. Therefore, it is critical to consider the plausible range of future tropical Pacific climate changes using models, observations, and theories, and to understand the broader implications of these changes. The question of how ENSO variability would respond to global warming has been addressed elsewhere<sup>1,3,4</sup> and so is not the focus of this paper. Instead, we review the plausible range of long-term future changes in the zonal SST gradient and Walker circulation within the equatorial Pacific region, based not only on model projections but also on observations and theories.

With this goal in mind, we first summarize modeling and observational studies that suggest differing trajectories for the tropical Pacific climate. Next, we describe hypothesized

<sup>1</sup>Department of Meteorology and Atmospheric Science, Pennsylvania State University, University Park, PA, USA. <sup>2</sup>Climate Prediction Center, National Oceanic and Atmospheric Administration, Maryland, MD, USA. <sup>3</sup>Geophysical Fluid Dynamics Laboratory, National Oceanic and Atmospheric Administration, Princeton, NJ, USA. <sup>4</sup>Lamont-Doherty Earth Observatory, Columbia University, New York, NY, USA. <sup>5</sup>Department of Earth, Atmospheric and Planetary Sciences, Massachusetts Institute of Technology, Cambridge, MA, USA. ✉email: [sxl31@psu.edu](mailto:sxl31@psu.edu)

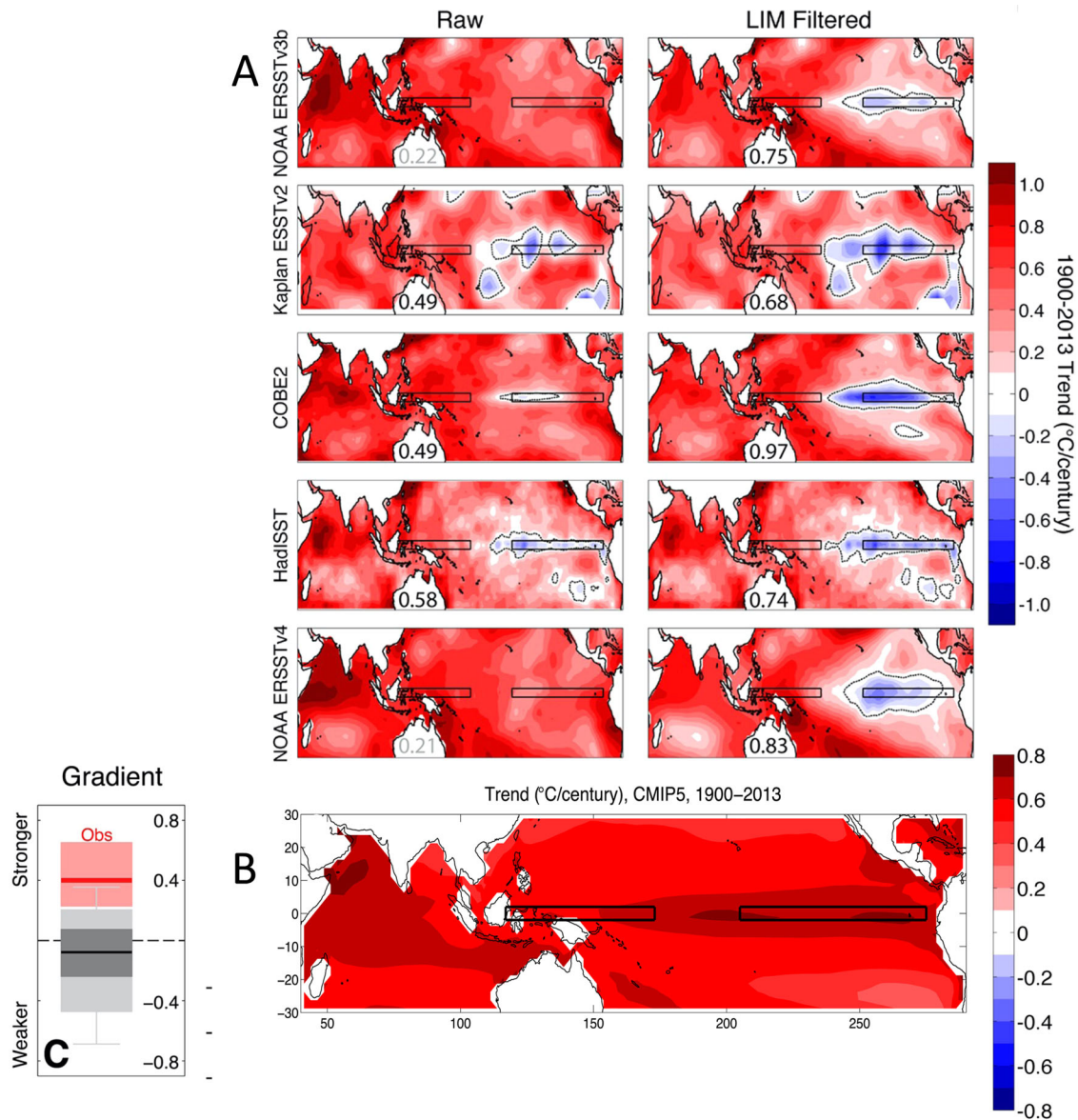


**Fig. 1** SST trend ( $^{\circ}\text{C}$  [100 yr] $^{-1}$ ) from 1900–2013. **A** observation-based data and **(B)** 83 CMIP5 simulations from 41 models with historical radiative forcing; RCP future projection values are used after 2005. In **(A)**, the SST reconstructions used for each panel are indicated on the y axis. Also in **(A)**, the left column shows the unfiltered trend and the right column shows the trend with linear El Niño–Southern Oscillation dynamics removed using an optimal perturbation filter<sup>199</sup>. The numbers in **(A)** are the values of the trend in the SST difference between the two boxes, one over the western tropical Pacific, and the other over the eastern tropical Pacific. The range of the CMIP5 trends ( $^{\circ}\text{C}/\text{century}$ ) is shown in **(C)**. These plots are adapted from ref. <sup>23</sup> which provides additional information on the data used.

mechanisms that would support either of these trajectories, and discuss the potential consequences of getting the future projections wrong. Lastly, we highlight research avenues that could help to improve and build confidence in future projections of tropical Pacific climate.

### OBSERVED AND SIMULATED TRENDS IN EQUATORIAL PACIFIC CLIMATE

Identifying observed trends in tropical Pacific climate is muddled by the varying methods, datasets, and time periods used. This section partitions the literature into studies that detect El Niño-like trends in tropical Pacific variables, those that predominantly identify La Niña-like trends, and studies arguing that the trends are mixed or that neither El Niño nor La Niña patterns project onto observed trends. Although not the basis for the classification

below, El Niño-like trends appear more often in studies emphasizing future long-term projections from models (e.g. from the Coupled Model Intercomparison Project (CMIP)), whereas La Niña-like trends are suggested more in studies prioritizing the recent historical observational-based data. Assessments of the tropical Pacific sensitivity to long-term climate change from observational records are limited by dataset uncertainties (especially prior to the 1950s<sup>5</sup>), and by the single real-world realization that is available to characterize externally-forced changes. Model projections have an advantage of providing longer records, larger ensembles, and multiple scenarios to assess the roles of individual forcings, while being limited by systematic (and often shared) model biases, such as an excessive equatorial Pacific cold tongue, a tendency towards a double Intertropical Convergence Zone (ITCZ) in the eastern Pacific, and an overly aggressive historical warming trend of the tropical upper troposphere<sup>6–8</sup>.

### “El Niño-like” trends toward weaker zonal gradients

Several studies<sup>9,10</sup> have provided a physical explanation for the El Niño-like response to increased greenhouse gases seen in coupled general circulation models (see the next section on theories for a fuller description). Observed SLP trends during 1861–1992 were analyzed and found to corroborate the projected reduction in strength of the Pacific Walker circulation<sup>11</sup>. The observed SLP trends were only reproduced in the GFDL CM2.1 model when anthropogenic forcing was imposed, suggesting that El Niño-like trends were a consequence of global warming. This conclusion was reinforced by all of the CMIP3 models evaluated in the IPCC AR4, which showed a weakening of the Walker circulation<sup>12</sup>.

Even with the discovery of long-term weakening trends in several different SLP datasets, discrepancies among the observational SST datasets over 1880–2005 were noted, with warming trends in the eastern Pacific in ERSST, and cooling trends in HadSST<sup>13,14</sup>. Ref. <sup>15</sup> also noted disagreements in the zonal SST gradient trends among observational SST datasets (ERSSTv3b<sup>16</sup>, HadISST<sup>17</sup>, ICOADS), but showed that using only bucket-sampled SSTs (to avoid biases caused by measuring temperatures at the ship engine intakes<sup>18</sup>) and nighttime marine air temperatures (to avoid the daytime heat island effect) revealed a weakening zonal SST gradient over the period 1950–2009. AGCMs forced by the merged bucket-nighttime SST dataset simulated a weakening Walker circulation<sup>19</sup>.

Despite uncertainties in the observational zonal SST gradient trend, most of the latest global warming projections from coupled climate models project a future weakening of the Pacific zonal SST gradient along the equator<sup>20,21</sup>. Historical CMIP simulations from 1950–2010 indicate SST warming that is most apparent near the equator, though there is a discernible shift in the location of peak warming from the western and central Pacific in CMIP3 to the eastern Pacific in CMIP5<sup>22</sup>. The appearance of a more El Niño-like SST trend pattern in CMIP5 and CMIP6 has been recognized in a number of studies<sup>1,2,23–27</sup>. An even stronger simulated El Niño-like pattern in SSTs and in the tropical atmospheric circulation appears when a statistical correction is applied to the CMIP5 RCP8.5 projections<sup>28–30</sup>, in an attempt to account for systematic errors among coupled models—including SSTs that are too cold in the central equatorial Pacific and too warm in the southeast tropical Pacific—which influence the simulated dynamical responses of the tropical Pacific to changing radiative forcings.

### La Niña-like trends toward stronger zonal gradients

Examining the 1900–1991 period using several oceanic datasets<sup>31–33</sup>, ref. <sup>34</sup> found a La Niña-like trend of cooling in the central-to-eastern Pacific Ocean and a strengthening of the western/central Pacific westward SST gradient. With the more recent expansion of observational datasets and a longer climate record, it appears that this overall tendency has continued through at least 2020<sup>2,35,36</sup>. Using some of the most frequently cited SST datasets (HadISST1<sup>17</sup>, Kaplan Extended SST<sup>33</sup>, ERSSTv3<sup>16</sup>, ref. <sup>37</sup> determined that the zonal SST gradient had strengthened from 1880 to 2005, most prominently during boreal fall and winter. SST datasets that include more recent time periods show the continuation of La Niña-like trends<sup>2,36</sup>. Analyses of companion SLP datasets (HadSLP2<sup>38</sup>, Kaplan SLP<sup>39</sup>, ERSLP<sup>40</sup>) showed disagreement in the zonal SLP gradient trend among the datasets, with HadSLP2 and Kaplan SLP suggesting weakening during the boreal spring, and ERSLP exhibiting no statistically significant trend for any season<sup>37</sup>. Upon removing the linear component of ENSO dynamics from various SST datasets using Linear Inverse Modeling (LIM), a more consistent strengthening of the SST gradient over 1900–2010 was discovered<sup>1</sup>. The LIM was used to filter out additional internal variability and resulted in more agreement in the trend among various SST datasets<sup>23</sup> (right panels of Fig. 1A).

In addition to SST, a closer examination of SLP records also pointed in the direction of La Niña-like trends for more recent decades, when the observations have better coverage and there is more agreement between datasets. An examination of SLP records for different lengths of time and different datasets revealed 30-year running trends toward higher (i.e. “El Niño-like”) SLP over Indonesia prior to the early 1970s, then followed by trends toward lower (i.e. “La Niña-like”) SLP afterward, with weaker opposite-signed SLP trends over the eastern Pacific Ocean<sup>5</sup>. Overall, SST and SLP trends can be sensitive to the datasets used, the duration examined, the spatial reference points for the gradient calculation, and the start and end dates<sup>5</sup>.

Enhanced observations over the past few decades allow for the analysis of trends in other variables beyond SST and SLP. Several studies<sup>41–43</sup> used satellite-based observations of precipitation, atmospheric moisture, and water vapor transports to identify a recent strengthening of the tropical Pacific Walker circulation. In a 30-year record from 1979–2008, a significant trend in the Pacific Walker circulation was identified in a number of interconnected variables – SST, SLP, and atmospheric convection, moisture, and winds in the boundary layer<sup>44</sup>. The strengthening of the Walker circulation was also inferred from observations of sea level (from satellite altimeters and tide gauges), and outgoing longwave radiation<sup>45–47</sup>. Over a similar period (1979–2012), the Pacific Walker circulation strengthened and shifted westward, and the La Niña-like trends in SST were enough to reproduce the trends in the Walker circulation in an associated set of simulations of an atmospheric model forced by observed SSTs<sup>48</sup>. While corroboration among multiple types of variables is helpful, trends over short epochs can also be strongly influenced by internal variability, particularly the decadal regime-like shifts in 1976/77 and 1997/98<sup>4,49,50</sup>. The impact of (known) internal variability on SST trends is further discussed below.

### El Niño- or La Niña-like Trends are Mixed, transient, or Not Sufficiently Clear

A study of a global warming scenario from 20 CMIP3 coupled climate models determined that the simulated future trends in the equatorial Pacific zonal SST gradient were neither robustly El Niño-like nor La Niña-like<sup>51</sup>. Models with more realistic representations of historically observed ENSO patterns (in terms of SST, SLP, and precipitation) also tended to produce smaller projected future trends in the equatorial Pacific zonal gradients.

In a coupled climate model simulation with radiative forcing instantaneously returned from present-day levels to preindustrial levels, it was inferred that the fast response to increasing greenhouse gases produces a more La Niña-like pattern with an enhanced zonal temperature gradient, while the slow response is more El Niño-like; similar conclusions have been drawn based on simulations with models subject to transient and/or abrupt CO<sub>2</sub> increases of varying magnitudes<sup>52,53</sup>. The slow response is calculated as the average of the 10–30 years following the forcing change, and the fast response is the difference between the slow response and the 20 years centered on the forcing change. In doubled CO<sub>2</sub> experiments, 7 out of 11 models considered by ref. <sup>54</sup> initially indicate La Niña-like changes that eventually become more El Niño-like. These model behaviors were interpreted as the oceanic thermostat being more pronounced on transient time-scales, because the eastern Pacific remains sensitive to cool upwelling waters that have not yet been affected by global warming<sup>52,54</sup>. The hypothesis is that in the initial stages of global warming, the eastern Pacific SST response is dominated by the increased vertical stratification of temperature, which acts through upwelling to inhibit warming of the surface. Eventually, however, this effect fades as warming surface waters subducted in the subtropics eventually reach the equatorial subsurface, weakening the stratification and warming the upwelling waters. This time-

dependent response is, however, by no means common in coupled models. If a transient La Niña-like response occurs in models then the tropical Pacific SST trends over recent decades, during which subsurface waters have warmed less than surface waters, should be La Niña-like. However, no models have the transient forced response that strengthen the zonal gradient by as much as observed over the 1958 to 2018 period (Fig. 4B).

### Role of internal variability

From the aforementioned studies, it is evident that most climate models simulate and project El Niño-like future trends, while most observational studies (on time spans longer than several decades to a century) point to La Niña-like historical trends, especially in recent decades. These observational trends are largely acknowledged, but whether they are radiatively forced or arise from internal variability continues to be intensely debated<sup>4</sup>. The well-measured record remains relatively short, and the natural climate variability of the Pacific is large. The tropical Pacific SST went through decadal regime-like transitions in the early 1940s, the mid-late 1970s and the late 1990s, with the intervening period being warmer in central and eastern tropical Pacific than the earlier and later periods<sup>55–57</sup>. Trends that place the 1970s in the middle of the period therefore show warming of the central to eastern equatorial Pacific<sup>58</sup> while those that place the late 1990s in the middle show cooling of the same region<sup>46</sup>. Because CMIP models simulate some tropical Pacific decadal variability<sup>4</sup>, it is possible to find agreement in model and observed trends for some time periods and some models<sup>26,59</sup>.

What is striking about the observed strengthening of the equatorial zonal SST gradient is that it is also persistent in trends calculated over centennial timescales. These longer epochs span several transitions in Pacific decadal variability, and so their trends are less likely to be influenced by natural decadal variability<sup>23,35,37,60</sup>. Trends over these longer periods show widespread SST warming over the tropical Pacific, but a narrow, equatorially-confined band with little warming, or even some cooling, in the

central to the eastern basin (Fig. 1A). The equatorial confinement of the lack of warming is distinct from the meridionally broader cooling that arises from cold phases of Pacific decadal variability<sup>55–57</sup>. The persistence of the zonal gradient strengthening in trends evaluated over long periods, and its distinct spatial pattern, suggest that it may arise from mechanisms other than those associated with natural decadal variability, e.g., a radiatively-forced response.

To assess whether the discrepancy between observed and simulated trends is attributable to internal variability, one can check whether the observed trends lie within the ensemble spread of coupled GCM simulations with historical radiative forcing, since each ensemble member potentially mimics the single realization provided by observations.

Ref. <sup>61</sup> concluded that observed 20- and 50-year trends in the zonal SST and SLP gradients remain within the spread spanned by climate models (preindustrial runs from CMIP5, and preindustrial and present-day integrations of the Kiel Climate Model), although the observational datasets would reflect a more extreme realization of the simulated internal variability. In another study, trends in several atmospheric and oceanic variables and datasets over varying 30-to-65-year spans were examined alongside the CESM large ensemble<sup>62</sup>. This study showed that the CESM was able to capture a strengthening zonal gradient in its members during 1979–2014, but not the observed intensity of the change. The strengthening SST gradient over 1951–2010 was shown to fall within large ensembles (Fig. 2), but that many of these same simulations then reverse sign—that is, project a weaker SST gradient into the future<sup>26</sup>. In general, it is rare within such ensembles to find a historical strengthening of the zonal SST gradient that is comparable to that observed over the past 50 years.

In contrast, other studies have concluded that observed trends are inconsistent with historical simulations. Among ~40 CMIP5 models (~80 members total), none strengthened the equatorial Pacific zonal SST gradient as much as observed over 1900–2013<sup>2</sup> (see Fig. 1). During 1958–2017, observed trends in the Niño-3.4 index (SST

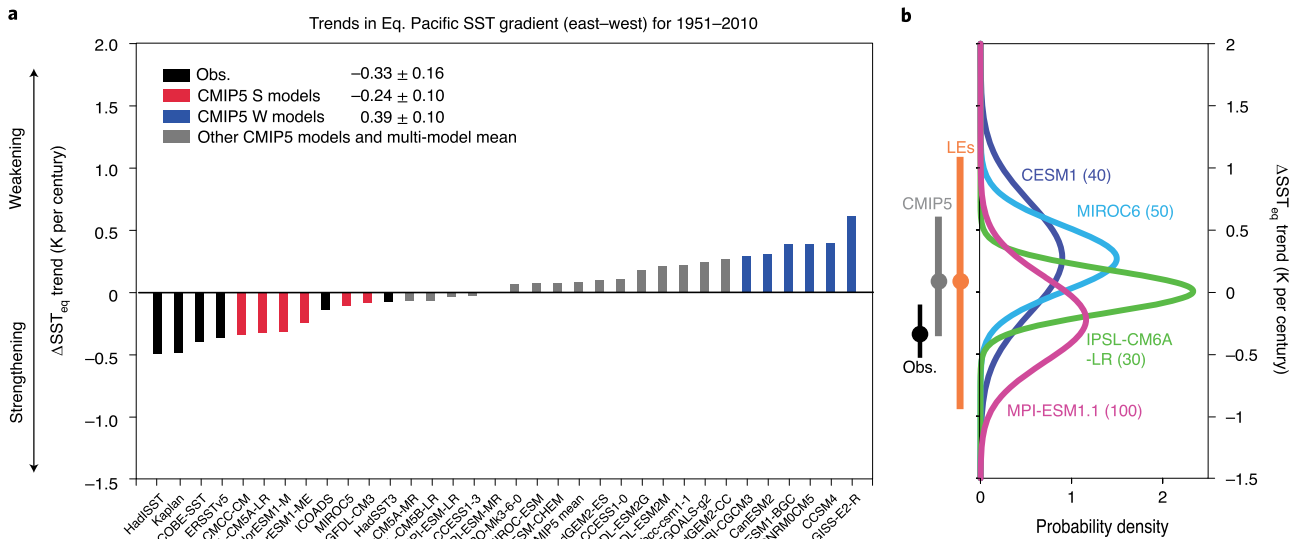


**Fig. 2** Equatorial Pacific zonal SST gradient trend during 1951–2010. **a** Linear trends for 1951–2010 of the equatorial Pacific zonal SST gradient, defined as the eastern Pacific (180°–80°W, 5°S–5°N) SST minus the western Pacific (110°E–180°, 5°S–5°N) SST from six observational data sources (Obs.), and 27 CMIP5 models. The S group (six models that show the largest magnitude of SST gradient strengthening) of CMIP5 models show a strengthening of the zonal SST gradient, and the W group (six models that show the largest magnitude of SST gradient weakening) of CMIP5 models show a weakening of the zonal SST gradient. **b** Probability density function of the 1951–2010 SST gradient trends in four large ensemble simulations indicated in the figure. The ensemble size is indicated in parentheses. Dots and bars in the left margin of **b** indicate the means and 5–95% ranges for the observations, CMIP5 models (one realization from each model) and combined large ensemble simulations. (Adapted from ref. <sup>26</sup>).

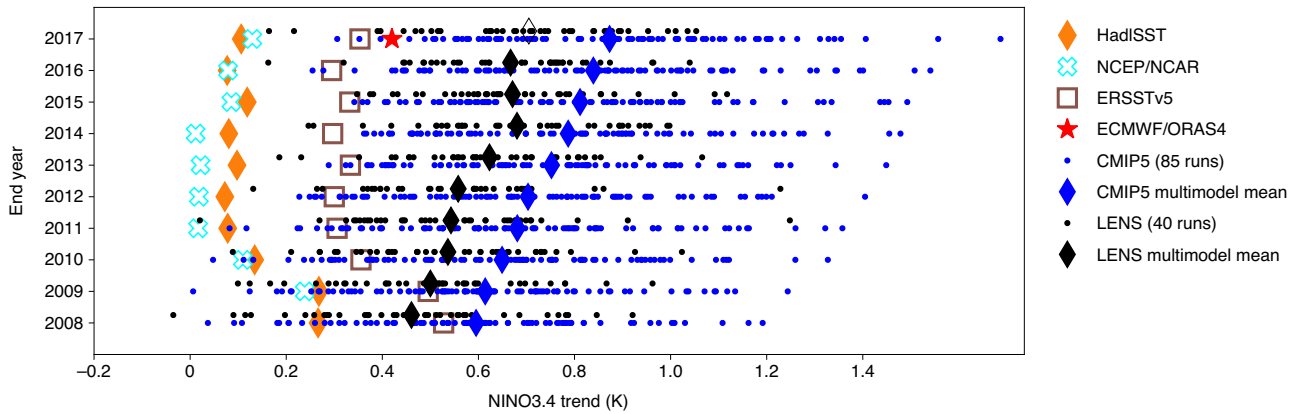


**Fig. 3** A comparison of observed and modeled SST trends in the Niño-3.4 region. The figure shows the distribution of 60-year trends in the Niño-3.4 region ( $5^{\circ}\text{S}$ – $5^{\circ}\text{N}$  and  $170^{\circ}\text{W}$ – $120^{\circ}\text{W}$ ) for end dates ranging from 2008–2017 for 88 individual CMIP5 model runs and 40 NCAR LENS runs. The CMIP5 and LENS multimodel means for each 60-year trend are also shown as blue and black diamonds. Also shown are the observational estimates from ECMWF, HadISST, National Centers for Environmental Prediction (NCEP)/NCAR and ERSSTv5 SST analyses. (Adapted from ref. 27).

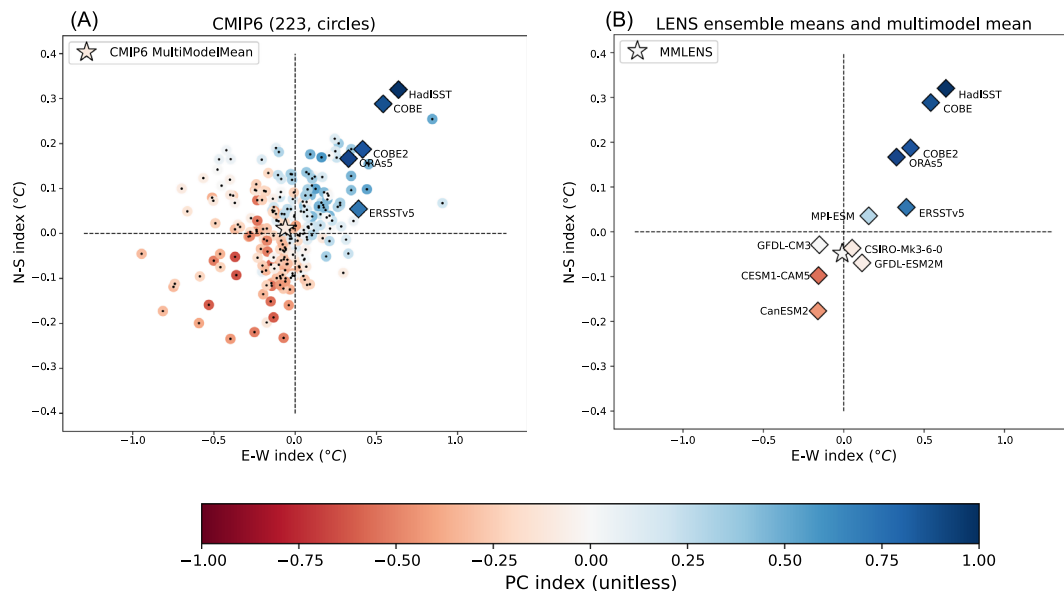


**Fig. 4** Tropical Pacific SST Trends from 1958 to 2018. Trends in the east-west SST gradient as measured by (a western box ( $140^{\circ}\text{E}$ – $170^{\circ}\text{E}$ ,  $3^{\circ}\text{S}$ – $3^{\circ}\text{N}$ ) minus an eastern box ( $170^{\circ}\text{W}$ – $90^{\circ}\text{W}$ ,  $3^{\circ}\text{S}$ – $3^{\circ}\text{N}$ ); horizontal axis), north-south near-equatorial SST gradient (the average of off-equatorial box ( $9^{\circ}\text{S}$ – $3^{\circ}\text{S}$ ,  $3^{\circ}\text{N}$ – $9^{\circ}\text{N}$ ) minus equatorial box ( $3^{\circ}\text{S}$ – $3^{\circ}\text{N}$ ) all for longitudes  $170^{\circ}\text{W}$ – $120^{\circ}\text{W}$ ; vertical axis), and the pattern correlation between the HadISST and simulated SST in the Pacific Ocean  $10^{\circ}\text{S}$ – $10^{\circ}\text{N}$  domain (color dots). **A** 511 individual realizations (colored dots) from 45 CMIP6 models, and the multimodel ensemble mean (white star); **B** Six multimodel LENS ensemble means (colored diamonds) and the six-model LENS ensemble mean (white star)<sup>2</sup>. Also shown in each panel are observation-based estimates from HadISST, COBE, COBE2, ERSSTv5, and ORAS5 (diamonds). Units for SST gradients are  $^{\circ}\text{C}$  per 61 years. This plot is adapted from ref. 2 (© American Meteorological Society. Used with permission.) which provides additional information on the data used and the methods.

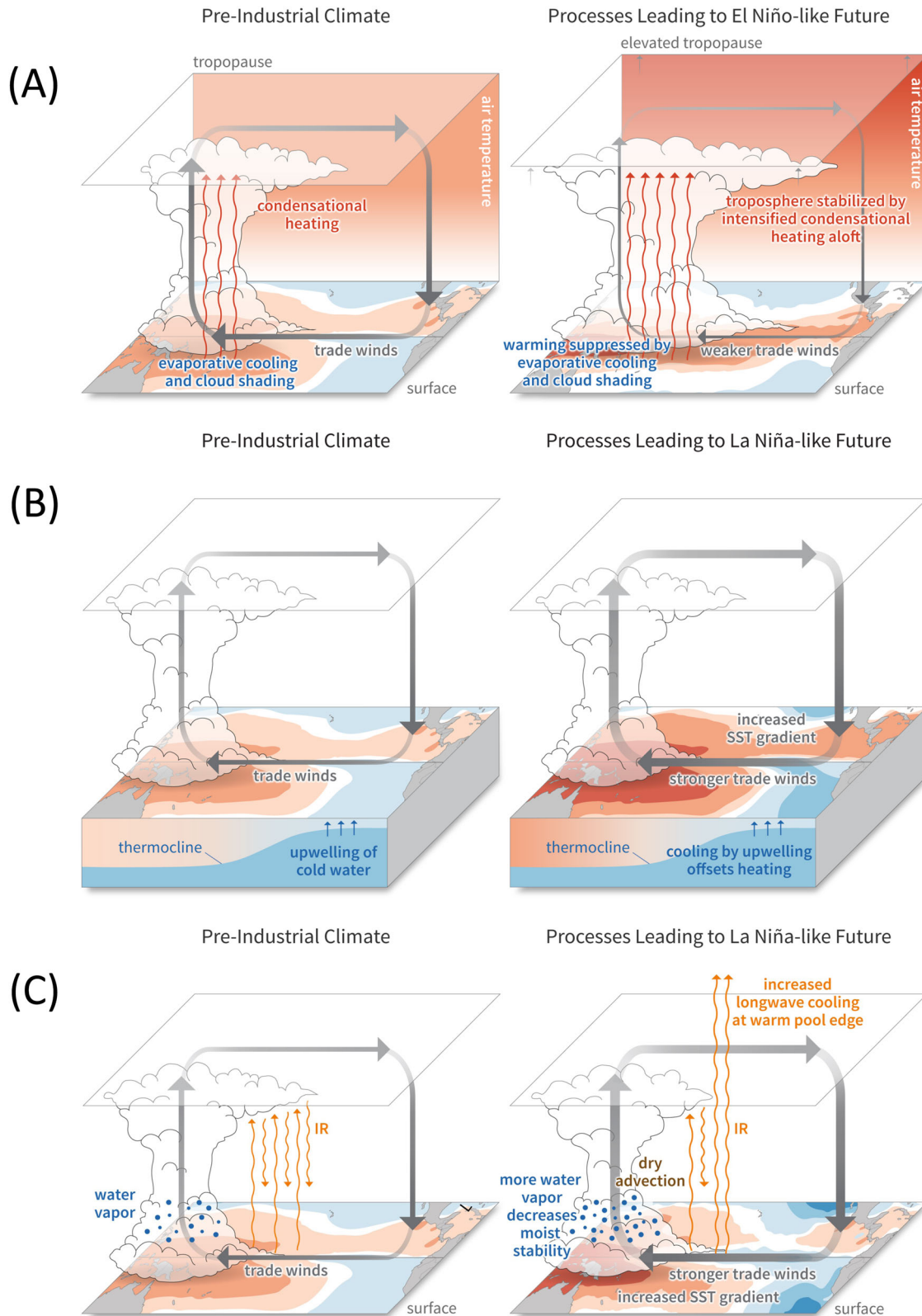
anomalies averaged over  $5^{\circ}\text{S}$ – $5^{\circ}\text{N}$  and  $170^{\circ}\text{W}$ – $120^{\circ}\text{W}$ ) lie either on the cold fringe, or entirely outside of, the spread of CMIP5 historical simulations<sup>27</sup> (Fig. 3). Discrepancies in the zonal SST gradient between the observed trends and model simulations persist in the CMIP6 models<sup>2</sup> (Fig. 4). Moreover, notable discrepancies were found between the observations and 35 runs of the NCAR Large Ensemble (LENS) project<sup>2,27</sup>. These analyses indicate that the observed SST trends ending in the current decade are at the very limit of the range of trends in individual CMIP5, CMIP6, and LENS model runs. The disparity between CMIP5 trends and the observational data has also been noted in the acceleration of the Pacific Walker circulation<sup>63</sup>. In a comparison of trends in the HadSLP2 observational dataset with 35 CMIP5 runs (forced by representative concentration pathways), it was found that none of the models produced a statistically significant acceleration in the Walker circulation like that observed during 1980–

2012<sup>64</sup>. The dissimilarity in SLP trends between the coupled models and observations was largest in the western equatorial Pacific.

### THEORIES FAVORING ENHANCED OR WEAKENED EQUATORIAL PACIFIC ZONAL SST GRADIENTS

#### Theories supporting a future El-Niño-like eastward expansion of atmospheric convection in the tropical Pacific

The first interpretations of the model-simulated tropical Pacific response to  $\text{CO}_2$  forcing were offered by ref. 9. In response to a 1% per year compounded  $\text{CO}_2$  increase, their coupled ocean-atmospheric model showed a 20% decrease in the equatorial zonal SST gradient, weaker easterly surface winds, and weaker ascent over the warm pool region. This weakening was despite a



15% increase in precipitation and latent heating in the rising branch of the Walker circulation. The weakening of the zonal SST gradient was explained in terms of the surface energy balance, with greater suppression of the surface warming in the West Pacific (where the background SST is warm, and so the surface

saturation water vapor pressure and evaporative cooling are more sensitive to SST changes) than in the East Pacific (where the background SST is cold)<sup>9,21,65</sup>. The weakening of the Walker circulation occurs despite increased tropospheric latent heating over the warm pool, due to increased dry static stability (static

**Fig. 5 Hypothesized processes leading to El Niño-like or La Niña-like future.** In each row, the left panel shows the processes in the pre-industrial climate and the right panel shows how those processes respond to greenhouse gas (GHG) warming and lead to changes in zonal asymmetry. These “seeds” of zonal asymmetry change grow, through the Bjerknes feedback, into a more El Niño-like or La Niña-like state. **A Left:** Convection is strongest in the western Pacific where the SST is the highest. Latent heating warms aloft, and evaporation cools the ocean surface. Right: SSTs in the tropical Pacific increase leading to more condensational heating aloft and a higher tropopause, which increases dry static stability and gross moist stability, thus weakening the Walker circulation. At the same time, evaporative cooling and cloud shading are more sensitive to warming in the western Pacific, which weakens the zonal SST gradient. **B Left:** As in the left panel of (A), except that the thermocline is shown. In the eastern Pacific, the thermocline is closest to the surface. Right: Under GHG warming, a uniform surface heat flux into the Pacific Ocean causes the SST to rise, but in the eastern tropical Pacific, the upwelling of cold water counters the forced warming. As a result, the zonal SST gradient increases. **C Left:** As in the left panel of (A), except it highlights the abundance of water vapor in the lower troposphere, and the trapping of infrared radiation (IR) by cirrus outflow from convective towers which otherwise escapes to space. Right: Under GHG warming, the lower troposphere becomes more moist which decreases the GMS and thus strengthens the Walker circulation. In the margins of the convective region, the horizontal moisture gradient increases, and advection from the surrounding drier region diminishes the area of convection. The so-called “iris effect” can also lead to a similar response to increased warming: Precipitation efficiency in convective tower increases, leaving less moisture for cirrus outflow. The resulting contraction of the cirrus cover in the periphery of the warm pool allows for more IR to escape, potentially cooling SSTs and thus enhancing the zonal SST gradient between the warm pool and its surroundings. Credit: climate.gov.

stability of unsaturated air), which strengthens the adiabatic vertical advective cooling for a given upward air velocity<sup>9</sup>. The dry static stability increases with warming due to increasing atmospheric humidity and the parameterization of moist convection, which removes convective instability and thus keeps the lapse rate close to the moist adiabatic rate. Due to the weak horizontal temperature gradients in the tropical free troposphere, the descending branches of the Walker and Hadley circulations also see increased static stability, and this reduces the subsidence needed to balance radiative cooling with adiabatic warming<sup>9</sup>. Thus, the atmospheric energy balance in both the ascending and descending regions is consistent with a reduced total overturning circulation in the tropical atmosphere. The evaporative cooling mechanism for a reduced zonal SST gradient and the static stability mechanism for a weakened Walker circulation are shown schematically in Fig. 5A. The atmospheric responses, however, may change over time as ocean heating starts to affect the SST pattern and the atmospheric circulation, as evidenced by the simulated asymmetric precipitation changes to CO<sub>2</sub> “ramp up” and “ramp down” experiments<sup>66</sup>. To the extent that these processes weaken the large-scale Walker circulation and surface easterly trade winds, the equatorial upwelling and the zonal tilt of the equatorial thermocline would also weaken, acting to further weaken the zonal SST gradient.

However, arguments based on increases in dry static stability do not provide a direct estimate of the change in strength of the Walker circulation, because both the latent heating and adiabatic vertical advective cooling terms in the atmospheric energy balance depend on the vertical velocity<sup>67</sup>. This may be taken into account by analyzing the moist static energy budget, and by considering the gross moist stability (GMS; a measure of the efficiency of circulations in exporting or importing energy<sup>68–70</sup>) instead of the dry static stability. In models, weakening of the Walker circulation is then found to be caused by an increase in GMS as the atmosphere warms, and this increase in GMS has been in turn related to the increase in the vertical depth of the circulation as the tropopause rises with warming<sup>67,71,72</sup> (Fig. 5A). However, the GMS is sensitive to how it is measured and defined, and the physical controls on it are not well understood since it depends on the vertical structure of the circulation, the thermal stratification and the relative humidity, and this limits confidence in theoretical predictions of a weakening Walker circulation with warming.

One of the robust responses in climate models to the doubling of CO<sub>2</sub> is the reduction in atmospheric convective mass fluxes<sup>10</sup>. Lower tropospheric water vapor increases with temperature according to the Clausius-Clapeyron rate if the relative humidity remains unchanged, while global mean precipitation (and tropospheric latent heating) increases with temperature at a much

slower rate (limited by how quickly the troposphere can cool itself, via outgoing longwave radiation or shortwave reflection from clouds)<sup>10</sup>. Meeting both constraints requires a reduced upward mass flux of moist air out of the boundary layer. A similar argument based on boundary-layer moisture balance and energetic constraints on evaporation has been made for reduced subsidence in regions of descent<sup>73</sup>. These theoretical interpretations<sup>9,10</sup> were used to argue that the total tropical overturning circulation, which includes the Walker circulation as a major component, should weaken with warming<sup>11</sup>. However, it was found that the Walker circulation strength is poorly correlated with the global convective mass flux suggested by ref. <sup>10</sup>; model-simulated Walker circulation responses appear to be determined more by the response of the models’ tropical Pacific zonal SST gradients, rather than their overall tropical warming<sup>74</sup>. Further, it has been argued that climate models would project even stronger El Niño-like responses were it not for model biases toward insufficient negative cloud-radiative feedbacks and excessive upper-oceanic meridional and zonal overturning in the equatorial Pacific<sup>29,30</sup>.

### Theories supporting a La Niña-like/zonally asymmetric convection response

The first theory in this category was proposed by ref. <sup>75</sup>, who pointed out the importance of ocean dynamics which had not been considered in prior studies of tropical temperature regulation mechanisms<sup>76–78</sup>. In the Zebiak-Cane model<sup>79</sup> of the tropical Pacific coupled ocean/atmosphere system, the SST evolves to a La Niña-like pattern in response to a spatially uniform imposed surface heat flux into the ocean<sup>75</sup>. Unlike in the western Pacific where the thermocline is deep, the continual upwelling of unperturbed cold water in the eastern equatorial Pacific counters the imposed surface warming there, thus amplifying the zonal SST gradient across the Pacific. This strengthens the Walker circulation, which further shoals the thermocline in the east, increases upwelling, and cools the cold tongue. This mechanism is schematically shown in Fig. 5B. In addition to this zonally asymmetric Bjerknes feedback, it was further argued that strengthened trade winds off the equator (in response to the increased SST contrasts) shoal the thermocline *all along* the equator in the Pacific which, again, leads to cooling at depth and in the cold tongue<sup>27</sup>. Ocean data and reanalyses do indeed show a trend towards thermocline shoaling consistent with this theory, although the shoaling could also have been caused in part by radiation-induced warming at the surface (caused by increased greenhouse gases) proceeding faster than advective-diffusive warming at depth.

In an idealized model of the Walker circulation designed to explore the role of different feedbacks, the Walker circulation

strengthens in response to a specified radiative flux divergence that mimics an increase in greenhouse gas loading<sup>80</sup>. The increased greenhouse gas loading causes stronger ascent in the convection region because the warmer and moister air decreases the GMS. In the margin of the convective region, advection from the surrounding drier region diminishes the area of convection<sup>80,81</sup>. This idea is illustrated in Fig. 5C. The decrease in GMS contrasts with the increase in GMS found in comprehensive climate models, and the discrepancy likely arises because the vertical structure of the circulation is not allowed to change with warming in the idealized model. Nonetheless, the results establish that the Walker circulation is sensitive to how GMS responds to warming (see “Toward more reliable projections of tropical Pacific SST change” for further discussion).

A different mechanism was proposed based on observations, but with the same result as in ref. <sup>80</sup>; the area of cirrus outflow from the deep convection region contracts as surface temperature increases<sup>82</sup>. This observations-based finding was interpreted as a consequence of a positive relationship between surface temperature and precipitation efficiency<sup>82</sup>. Because cirrus clouds trap outgoing longwave radiation more effectively than they reflect incoming shortwave radiation<sup>83</sup>, the shrinking of the cirrus area means more net radiative cooling, the so-called “iris effect”. If in a warmer world the cirrus area contracts to the warmest water, this would also dry and cool the margin of the convective region, hence increasing the zonal SST gradient (Fig. 5C). However, cirrus clouds also reduce surface downward shortwave irradiance, so this shortwave radiative forcing would warm those same cooler

waters. Since the tropospheric temperatures are coupled to the surface (by radiative fluxes, and by convective fluxes in regions of convection), how these longwave and shortwave radiative forcings play out in the fully coupled system remains uncertain. Therefore, their effects on SST gradients are not immediately clear. Further, whether the iris effect occurs in nature has been questioned in some studies<sup>84–86</sup> while other studies are supportive of its relevance<sup>87–89</sup>. Nevertheless, when an iris effect was imposed in an ad-hoc manner in a climate model, a more La Niña-like SST and precipitation response was simulated<sup>90</sup>. (Supplementary Figs. 6 and 16 in ref. <sup>90</sup> show that an increase in the iris effect results in more La Niña-like SST and precipitation changes).

There is also a theory supporting a La Niña-like response based on backward reasoning from a global constraint. Paleoclimate proxy data indicate that during past epochs when the global climate was warm, the Arctic was much warmer while tropical temperatures were comparable to current values. A number of different theories have been proposed to account for the wide range of equator-to-pole temperature gradients that have existed throughout Earth’s history. One of these theories is based on atmospheric dynamics<sup>91</sup>. Maintaining Arctic warmth against increased longwave cooling to space would require more heat influx from lower latitudes. In the atmosphere, midlatitude synoptic-scale waves cannot provide this additional heat transport, because they weaken as the pole-to-equator temperature gradient weakens. Instead, planetary-scale Rossby waves can provide the required heat transport because their strength is independent of the meridional temperature gradient. Under

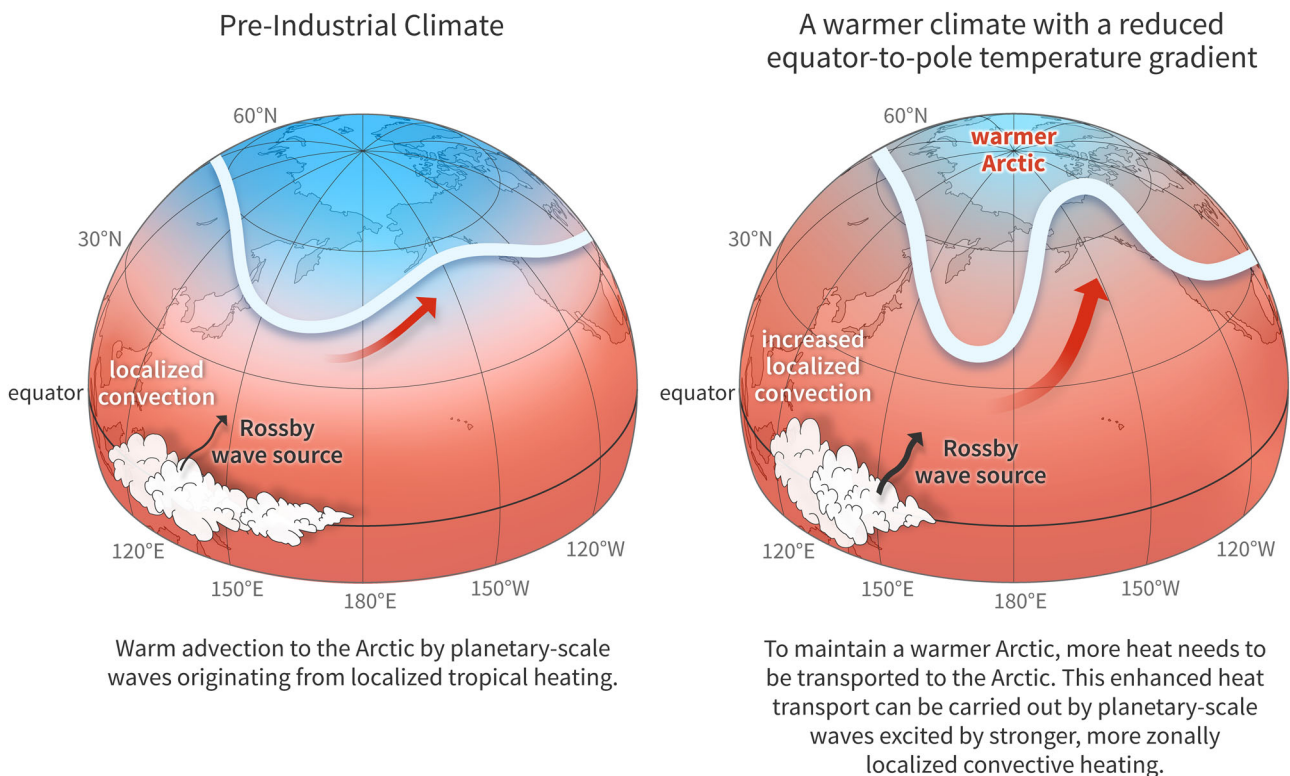


**Fig. 6 Mechanism favoring a La Niña-like condition from a general circulation perspective.** *Left:* On average, the strongest convection/rainfall occurs over Indonesia/Maritime Continent. The divergent circulation, resulting from the convection, advects absolute vorticity poleward. This leads to the generation of planetary-scale Rossby waves in the subtropics<sup>200</sup> that can propagate poleward and then upward once they reach mid- and high-latitudes. As these waves propagate upward, they transport heat poleward, which warms the Arctic. *Right:* Paleo-climate data suggests that when the global climate was warmer than today’s climate, the Arctic was considerably warmer while the tropics were about the same temperature as today’s climate. The higher Arctic temperature implies that longwave cooling to space must have been greater as well. To maintain the warmth against the increased longwave cooling, more heat needs to be transported from lower latitudes. Amongst the various atmospheric processes, the most probable candidate that can generate a stronger poleward heat transport in the face of a weakened meridional temperature gradient is a more enhanced tropical heating/convection around the Maritime continent, which is suggestive of a more La Niña-like pattern in convective heating and SST. Credit: climate.gov.



typical winter conditions, planetary-scale waves can propagate vertically throughout the troposphere and into the stratosphere<sup>92</sup>, transporting heat poleward and warming the Arctic. These planetary-scale waves can be excited by topography or by zonally varying latent heating, with the latter a more likely candidate since topography did not change systematically with respect to the meridional temperature gradient over past warm periods. Enhanced zonal asymmetries in tropical heating associated with a stronger zonal SST gradient in the Pacific are thus a probable candidate for maintaining the weak meridional temperature gradient during warm periods<sup>91</sup>. This idea is schematically shown in Fig. 6. This mechanism seems to have operated in the ongoing climate change of the past several decades<sup>93</sup> and also in intraseasonal time scale variability<sup>94,95</sup>. In addition, climate model simulations for the warm Cretaceous period show that a localization of tropical convective heating, with no change in tropical mean convective heating, can warm the Arctic by as much as 16 °C<sup>96</sup>. However, studies based on paleo proxy records do not definitely speak to one response or the other to global-mean warming, with some suggesting El Niño-like states<sup>97–100</sup> and others La Niña-like states<sup>101–105</sup>.

The theories mentioned in this section may not form a complete list. Additional processes deserving future investigation, that could potentially argue for either weakening or strengthening of the zonal SST gradient, include stratus cloud radiative feedbacks and land-sea interactions.

## CONSEQUENCES OF EQUATORIAL PACIFIC SST TRENDS

### Long-term impacts of changes in tropical Pacific time-mean SST

Future warming of the tropics-wide SST is projected to profoundly affect the climate of the global atmosphere and oceans. Warmer tropical SSTs will increase the specific humidity of the tropical atmospheric boundary layer, thereby increasing the moisture convergence for a given level of surface wind convergence, intensifying rainfall in convective zones (a “wet get wetter” pattern), and increasing the latent heating of the tropical troposphere. This leading-order response, however, may be substantially modified by changes in SST gradients—with zones of greater warming seeing increased rainfall, and zones of lesser warming seeing reduced rainfall, i.e. a “warmer get wetter” pattern of change over the tropical oceans<sup>21</sup>. This “warmer get wetter” pattern occurs as the troposphere becomes more unstable to convection in regions where there is an increase in relative SST (RSST, namely the local SST minus the tropical-mean SST). In addition to the effect of RSST on stability and convection, changes in horizontal SST gradients influence air temperature in the boundary layer and thus can drive changes in surface pressure gradients that affect the low-level circulation<sup>106,107</sup>. The resulting changes in surface convergence are roughly proportional to the Laplacian of the SST warming pattern and strongly affect rainfall in what has been termed a “Laplacian of warming” mechanism<sup>108</sup>. Thus, both the local and remote patterns of future SST change, and changes in tropical Pacific zonal and meridional SST gradients in particular, remain critical for determining the atmospheric response. For example, most CMIP models project future warming of the equatorial cold tongue relative to the rest of the tropics, shifting the Pacific Intertropical Convergence Zone (ITCZ) equatorward, resulting in more precipitation at the equator and less north of the equator<sup>109</sup>. Although not the focus of this review, inter-basin differences in the SST response are also an important factor when considering the stability of the tropical Pacific troposphere<sup>12,110,111</sup>. For example, a model that warms the tropical Pacific more than the tropical Indian and Atlantic, as opposed to vice versa, would be expected to see a greater increase in tropical

Pacific rainfall, even with identical changes in SST gradients within the tropical Pacific.

Future SST changes within the tropical Pacific could well differ from historically observed ENSO events. The details of the tropical Pacific SST changes matter, as demonstrated by the observed inter-event diversity of ENSO’s SST anomaly patterns and impacts<sup>112</sup>; for example, the 2015–16 El Niño produced a very different SST pattern and impacts than previous observed events<sup>113–115</sup>. Atmospheric deep convection tends to follow the warmest relative SST, and so future convectively driven teleconnections will depend on precisely how future warming alters the background time-mean pattern of SST<sup>21</sup>. The central Pacific is close to the SST threshold for convection; a slight change in the warming of that region could have an outsized impact on the locations of deep convection<sup>116</sup>, and thus on the atmospheric circulation and global hydroclimate<sup>117,118</sup>. Departures from historical norms would also impact seasonal predictions of ENSO and associated teleconnections, which are partially informed by statistical models trained on past observations<sup>119</sup>.

Even were the future change in climatological SST to resemble an ENSO pattern, its impacts could still differ from the impacts conventionally associated with seasonal-to-interannual ENSO variability. ENSO events tend to be synchronized to the seasonal cycle<sup>120,121</sup>, and their impacts are mediated by seasonally-dependent teleconnection mechanisms and local conditions — e.g. the upper- and lower-level jets and storm tracks, seasonal temperatures and precipitation, monsoons, and the local growing season<sup>115,122–126</sup>. A climatological change in the tropical Pacific that is sustained throughout the calendar year may thus have additional impacts beyond society’s experience with seasonally synchronized ENSO events. In addition, historical ENSO events have typically lasted no more than one or two years, allowing impacted systems to recover before the next event. An ENSO-like SST pattern that is sustained for decades or longer could expose ecosystems and societies to unprecedented stresses, requiring new modes of adaptation.

Potential impacts of future tropical Pacific SST changes on weather and climate risks can be gleaned from past ENSO events, which have altered global patterns of tropical cyclone formation<sup>127,128</sup>, seasonal temperatures, rainfall, and severe weather and hydroclimate events<sup>126,129</sup>. On longer time scales, the 1998–2015 La Niña-like time-mean SST pattern in the central and eastern equatorial Pacific has been linked to a strengthening of the Walker circulation, greater global ocean heat uptake, and prolonged drought over the southern U.S.<sup>130,131</sup> and in East Africa<sup>132,133</sup>. These changes cause worldwide disruptions to agriculture, ecosystems, and human health<sup>124,134,135</sup>. The trade winds also control the slope of sea level between the western and eastern tropical Pacific, influencing coastal ecosystems, ocean biogeochemistry, and infrastructure<sup>136,137</sup>. Changes in tropical Pacific SST thus have severe consequences for the world’s ecosystems and economies. The global economic impacts of the 1997–98 El Niño, for example, were estimated at \$32–96 billion<sup>138</sup>, with more than 20,000 deaths worldwide<sup>139</sup>. Reliable projections of future tropical Pacific SST change are thus critical to aid society in planning for adaptation.

ENSO variability also influences air-sea fluxes of CO<sub>2</sub> into the tropical Pacific Ocean, and the land-atmosphere fluxes of CO<sub>2</sub> worldwide<sup>140,141</sup>. Hence an ENSO-like pattern of tropical Pacific SST change would likely initiate climate-carbon feedbacks. However, given the involvement of changes in winds, SST, upwelling, and thermocline structure and depth, and the involvement of biogeochemical processes as well, it is not obvious what the implications of model biases might be for these feedbacks.

## Impacts of changing tropical Pacific SST on climate variability and associated risks

Future changes in tropical Pacific SST will have impacts beyond the time-mean climate, affecting modes of tropical Pacific variability. ENSO is influenced by the background pattern of tropical Pacific SST, with historical simulations and future projections demonstrating the impacts of the climatological SST on ENSO's amplitude, period, seasonal timing, duration, asymmetry, zonal propagation, and rainfall extremes<sup>1,3,142–148</sup>. A future “El Niño-like” reduction in the time-mean warm pool/cold tongue SST contrast would aid eastward and equatorward shifts of deep convection during El Niño, increasing the coupling of the Pacific convection and trade winds to ENSO SST anomalies, and amplifying ENSO rainfall anomalies and air-sea feedbacks<sup>3,145,149</sup>. A future “La Niña-like” time-mean response, with the thermocline shoaling in the east Pacific, could also increase ENSO amplitude, but through a different mechanism —namely a stronger background vertical temperature gradient in the cold tongue, which would amplify seasonal-scale SST anomalies induced by anomalous upwelling<sup>150</sup>; although this effect could be offset by other processes<sup>151</sup>.

Competing changes in ENSO feedbacks and forcings, and their complex sensitivities to background SST changes and model biases, are the main sources of uncertainty in climate model projections of future ENSO behavior<sup>28–30,143,152–155</sup>. In particular, ENSO's cloud feedbacks are underestimated in most models, due to the models' overly cold SST in the eastern equatorial Pacific<sup>156,157</sup> which reduces confidence in future projections of ENSO's SST patterns and rainfall extremes<sup>155</sup>. This underscores the importance of ongoing efforts by modelers to diagnose, reduce, and mitigate model biases<sup>144,158,159</sup>, in order to support more accurate projections of future tropical Pacific SST changes and their impacts on ENSO.

These tropical errors also have consequences for global estimates of climate sensitivity, the so-called “pattern effect,” which identifies SST anomalies in the Indo-Pacific as especially key for understanding radiative feedbacks<sup>160,161</sup>. Larger positive cloud feedbacks are associated with a decrease in the zonal gradient of SST across the tropical Pacific Ocean, owing in large part to the reduction of inversion strength and low cloud cover in regions dominated by subsidence<sup>162,163</sup>. Additionally, if surface warming is enhanced in regions that lack deep atmospheric convection, such as the eastern equatorial Pacific, then the lapse rate feedback would be reduced, further increasing the climate sensitivity for a tropical Pacific SST trend pattern that reduces the zonal SST gradient<sup>164</sup>. However, a pattern of tropical Pacific warming that enhances the zonal SST gradient, as in the historical record, produces stronger negative radiative feedbacks and a smaller equilibrium climate sensitivity than in models forced with an increase in anthropogenic emissions and that reduce the Pacific zonal SST gradient<sup>161,165</sup>. Thus, constraining the pattern of tropical Pacific SST change, and associated cloud and lapse rate feedbacks, is key to determining the rate of global mean warming in the future.

Future changes in the background tropical Pacific SST pattern, by modifying air-sea feedbacks, variability, and convective forcing of the atmosphere, could in turn alter ENSO's remote teleconnections and impacts. As described earlier, much of the uncertainty regarding ENSO's future behavior stems from the wide range of projected future tropical Pacific climatological SST patterns; models that project greater warming in the central equatorial Pacific also exhibit greater future extremes of rainfall and convective heating in that region<sup>1,155</sup>. These changes in tropical Pacific forcing patterns may also amplify, weaken, or displace longstanding historical teleconnections, in addition to the shifts in teleconnection pathways arising from climate changes outside of the tropical Pacific<sup>129,166–168</sup>. The sensitivity of remote extremes

and impacts to differences in the tropical Pacific SST projections can be strongly region-dependent and nonlinear<sup>166,169,170</sup>.

Biases in the models' background climatological SSTs have also been implicated in problems simulating decadal-scale inter-basin interactions and their role in future climate change<sup>4,171,172</sup>. In that vein, SST projection biases might alter the role of future inter-basin interactions in model-projected climate risks. For example, the intensity of the intraseasonal Madden-Julian Oscillation (MJO), which modulates extreme weather events around the globe, is strongly related to both the background SST gradients and the tropospheric static stability set by the tropical-mean SST. Model studies have shown a strong sensitivity of the MJO to the tropical SST trend pattern, with regions of greater future SST warming showing greater increases in MJO precipitation variability<sup>173,174</sup>. Whether the equatorial Pacific cold tongue SST warms relative to the rest of the tropics will also likely have impacts on tropical cyclone formation and development, akin to those observed during ENSO events<sup>175</sup>. The weakened cold tongue pattern seen in CMIP projections, if erroneous, could result in a misleading projected trend towards fewer Atlantic tropical cyclones.

Projections of future tropical Pacific SSTs also hold implications for ocean observing<sup>176,177</sup>. Regions that are expected to change more rapidly may be prime candidates for sustained and enhanced observing, since these regions may be among the first to display changes that are robustly detectable against the background of natural climate variability, and that can be attributed to anthropogenic forcing. Existing observations already indicate that recent warming of the western equatorial Pacific SST has emerged as a clearly detectable forced change, in terms of both the mean climate and the interannual extremes<sup>114,178</sup>. Reliable projections of tropical Pacific changes are needed to inform the redesign of the Tropical Pacific Observing System (TPOS), which is now underway to enhance measurements and understanding of this critical region<sup>177</sup>.

There is recent evidence that, in initialized seasonal climate prediction models, El Niño false alarms have increased in the last half of the 1982–2020 record<sup>179</sup>, and this may be tied to errors in simulated linear SST trends across the equatorial Pacific Ocean<sup>36,180</sup>. As described earlier, many state-of-the-art seasonal climate prediction models have stronger positive trends in the central and eastern tropical Pacific than found in the observations. The emergence of SST trend errors in monthly and seasonal predictions further motivate understanding and constraining future projections of tropical Pacific climate – because identifying sources of uncertainty could yield immediate, near-term benefits for subseasonal-to-seasonal climate forecasts.

## TOWARD MORE RELIABLE PROJECTIONS OF TROPICAL PACIFIC SST CHANGE

### What aspects of models need to be improved?

Theory suggests that the response of the Walker circulation to climate warming is sensitive to changes in tropospheric thermal stratification in the tropics. It is clear from observations that the upper troposphere has been warming faster than the surface, consistent with climate-model projections<sup>181</sup>. In recent decades models appear to have simulated more upper-tropospheric warming than observed<sup>7,182</sup> which could overly weaken their Walker circulations<sup>183</sup> and warm the eastern tropical Pacific SSTs. Excessive warming of eastern tropical Pacific SSTs, in turn, could have further contributed to the upper tropospheric warming<sup>7</sup>, exacerbating the warming biases and the weakening of the Walker circulation. This model-observations discrepancy has been explained in terms of the recent phasing of Pacific decadal variability that has prevented warming in the central to eastern tropical Pacific<sup>184</sup>. Furthermore, it has been argued that the most relevant measure of stratification for Walker circulation strength is

the GMS rather than the dry static stability<sup>67,71,72</sup>. Changes in GMS are sensitive to changes in relative humidity and the vertical structure of the circulation, in addition to the vertical structure of warming, and contribute to much of the intermodel scatter in Walker circulation response in CMIP6 models from an energy budget perspective<sup>185</sup>. Improving simulations of changes in tropical stratification and humidity will depend on better understanding and representing convection in parameterizations<sup>186</sup>, global cloud-resolving simulations<sup>187</sup>, or data-driven convective parameterizations learned from high-resolution simulations<sup>188–190</sup>.

On the ocean side, surface heat flux feedbacks<sup>9</sup> can be invoked to help explain why CMIP models tend to have enhanced warming in the cold tongue. Due to the chronic excessive cold tongue and double ITCZ biases which have persisted in each generation of models, the eastern equatorial Pacific has higher surface relative humidity and lower wind speeds and SST than observed<sup>27</sup>. Both of these biases weaken the inhibition of SST changes by evaporative cooling and cloud shading, thereby enhancing the cold tongue SST sensitivity to radiative forcing — i.e. more warming of SSTs is required for the increased latent heat flux and cloud shading to balance the increased downward longwave radiation arising from a strengthened greenhouse effect. In addition, misrepresentations of SSTs in the extratropics, such as Southern Ocean SST, can also influence the zonal gradient of the tropical Pacific SST<sup>191</sup>. A simple atmosphere-ocean model with a prescribed climatology responded to the historical increase in greenhouse gases with an *enhanced* zonal SST gradient when the *observed* climatology was imposed, but a *reduced* gradient when the *CMIP5 multi-model mean* climatology was imposed<sup>27</sup>. Climate models with higher oceanic resolution appear to simulate more accurate equatorial Pacific SST and ENSO patterns, but the increasing atmospheric resolution still results in persistent errors in radiative flux feedbacks<sup>192</sup>. This emphasizes the need for the climate community to invest in reducing the tropical SST and circulation biases endemic to multiple generations of CMIP class models.

There are likely other aspects of climate models that could be as important for improving the accuracy of future projections of tropical Pacific SST. One approach to identify these potentially important deficiencies could be to link the reliability of seasonal forecasts to the slower multidecadal-to-centennial forced climate response<sup>193</sup>. Errors that emerge in a 2-day forecasts are often similar to the time-mean systematic errors simulated by the models<sup>194,195</sup>, indicating that some model errors are established very quickly. Initialized model hindcasts, coupled with real-time forecasts, could offer more rapid assessments of potential errors<sup>36,180</sup> and provide additional physical insights if the same models are also used for long-term projections. Because causality can be more readily diagnosed by examining time evolution, identifying long-term model errors that emerge on subseasonal-to-seasonal time scales<sup>195,196</sup> provides excellent opportunities for process studies to improve the accuracy of model projections.

### How should users weigh model projections and observations in their decision-making?

Climate models have been extensively used for climate risk mitigation planning. In contrast, observational trends that deviate from model consensus projections have been widely regarded as being caused by internal variability, and hence have not been considered for climate risk assessments. However, given the possibility that observed tropical Pacific SST trends that deviate from the model consensus projection might include a forced response, observed SST trends should also be considered when assessing climate risks. Faced with this emerging evidence, not taking observed trajectories into consideration increases the possibility of making a type 2 error, i.e. a missed warning<sup>197</sup>.

In the face of low confidence in future projections of tropical Pacific climate, a storyline approach<sup>197,198</sup> could provide a pathway for describing risks to users. Storylines are built from conditional statements, such as: “If a certain regional climate change were to occur, what would be the consequences of that event?” Applied to the current debate, planners can outline different possibilities guided by both model projections and observational trajectories. For example, “If the La Niña-like trend continues, then water resources in the southern tier of the U.S. may need to be reinforced to prepare for increased drought.” Or “If El Niño-like trends were to emerge as the models predict, then the Pacific Northwest may need to take steps to get ready for a drier future”.

## SUMMARY AND FUTURE OUTLOOK

We have reviewed the evidence that there are significant divergences between observations and model simulations of historical changes in the zonal contrasts of tropical Pacific climate. Theories exist that support the model projections and argue that the zonal SST gradient should weaken while other theories are consistent with the observed trajectories and argue that the zonal SST gradient should strengthen.

All of these theories have limitations and are incomplete. Further, the tropical Pacific is a region of strong natural variability, which might be obscuring the forced response in nature. Given the weaknesses of models in the tropical Pacific, it is important to pay serious attention to the observational record. The challenge ahead is to determine whether the observed record of a strengthening zonal SST gradient is indeed a forced response, or a product of natural variability on decadal and longer timescales, or perhaps even misleading due to data and sampling problems. Next, if it can be deduced that the observed strengthening is indeed forced, then why is it not simulated by climate models? Alternatively, if it can be concluded that the observed record is dominated by natural variability, can models reproduce this variability, and when will a forced signal emerge? Answering these questions requires a fundamental analysis of mechanisms of variability and change in observations and models, considering all the relevant physical processes. This work must be open to the idea that climate models, as currently formulated, may be deficient in their representations of past and future changes in tropical Pacific climate. Until this issue is resolved, many aspects of future projections that are strongly influenced by the tropical Pacific – including future regional climate, teleconnected climate risks, and the oceanic uptake of CO<sub>2</sub> – will be highly uncertain.

## DATA AVAILABILITY

Data sharing not applicable because no datasets were generated or analyzed for this article.

## CODE AVAILABILITY

Code sharing not applicable because no calculations were performed for this article.

Received: 17 March 2022; Accepted: 30 September 2022;

Published online: 31 October 2022

## REFERENCES

1. Cai, W. et al. Changing El Niño–Southern Oscillation in a warming climate. *Nat. Rev. Earth Environ.* **2**, 628–644 (2021).
2. Seager, R., Henderson, N. & Cane, M. Persistent Discrepancies between Observed and Modeled Trends in the Tropical Pacific Ocean. *J. Clim.* **35**, 4571–4584 (2022).
3. Cai, W. et al. In El Niño Southern Oscillation in a Changing Climate 289–307 (2020).

4. Power, S. et al. Decadal climate variability in the tropical Pacific: Characteristics, causes, predictability, and prospects. *Science* **374**, eaay9165 (2021).
5. L'Heureux, M. L., Lee, S. & Lyon, B. Recent multidecadal strengthening of the Walker circulation across the tropical Pacific. *Nat. Clim. Change* **3**, 571–576 (2013).
6. Fu, Q., Manabe, S. & Johanson, C. M. On the warming in the tropical upper troposphere: Models versus observations. *Geophys. Res. Lett.* **38**, L048101 (2011).
7. Mitchell, D. M., Eunice Lo, Y. T., Seviour, W. J. M., Haimberger, L. & Polvani, L. M. The vertical profile of recent tropical temperature trends: Persistent model biases in the context of internal variability. *Environ. Res. Lett.* **15**, 1040b1044 (2020).
8. Bao, J., Stevens, B., Kluff, L. & Jiménez-de-la-Cuesta, D. Changes in the Tropical Lapse Rate due to Entrainment and Their Impact on Climate Sensitivity. *Geophys. Res. Lett.* **48**, e2021GL094969 (2021).
9. Knutson, T. R. & Manabe, S. Time-Mean Response over the Tropical Pacific to Increased CO<sub>2</sub> in a Coupled Ocean-Atmosphere Model. *J. Clim.* **8**, 2181–2199 (1995).
10. Held, I. M. & Soden, B. J. Robust Responses of the Hydrological Cycle to Global Warming. *J. Clim.* **19**, 5686–5699 (2006).
11. Vecchi, G. A. et al. Weakening of tropical Pacific atmospheric circulation due to anthropogenic forcing. *Nature* **441**, 73–76 (2006).
12. Vecchi, G. A. & Soden, B. J. Global warming and the weakening of the tropical circulation. *J. Clim.* **20**, 4316–4340 (2007).
13. Vecchi, G. A., Clement, A. & Soden, B. J. Examining the tropical Pacific's response to global warming. *Eos, Trans. Am. Geophys. Union* **89**, 81–83 (2008).
14. Deser, C., Alexander, M. A., Xie, S.-P. & Phillips, A. S. Sea surface temperature variability: patterns and mechanisms. *Annu. Rev. Mar. Sci.* **2**, 115–143 (2010).
15. Tokinaga, H., Xie, S.-P., Deser, C., Kosaka, Y. & Okumura, Y. M. Slowdown of the Walker circulation driven by tropical Indo-Pacific warming. *Nature* **491**, 439–443 (2012a).
16. Smith, T. M., Reynolds, R. W., Peterson, T. C. & Lawrimore, J. Improvements to NOAA's Historical Merged Land & Ocean Surface Temperature Analysis (1880? 2006). *J. Clim.* **21**, 2283–2296 (2008).
17. Rayner, N. A. et al. Global analyses of sea surface temperature, sea ice, and night marine air temperature since the late nineteenth century. *J. Geophys. Res.: Atmos* **108**, 2670 (2003).
18. Kent, E. C. & Taylor, P. K. Toward Estimating Climatic Trends in SST. Part I: Methods of Measurement. *J. Atmos. Ocean. Technol.* **23**, 464–475 (2006).
19. Tokinaga, H. et al. Regional Patterns of Tropical Indo-Pacific Climate Change: Evidence of the Walker Circulation Weakening. *J. Clim.* **25**, 1689–1710 (2012b).
20. Liu, Z., Vavrus, S., He, F., Wen, N. & Zhong, Y. Rethinking Tropical Ocean Response to Global Warming: The Enhanced Equatorial Warming. *J. Clim.* **18**, 4684–4700 (2005).
21. Xie, S.-P. et al. Global Warming Pattern Formation: Sea Surface Temperature and Rainfall. *J. Clim.* **23**, 966–986 (2010).
22. Yeh, S.-W., Ham, Y.-G. & Lee, J.-Y. Changes in the Tropical Pacific SST Trend from CMIP3 to CMIP5 and Its Implication of ENSO. *J. Clim.* **25**, 7764–7771 (2012).
23. Coats, S. & Karnauskas, K. B. Are Simulated and Observed Twentieth Century Tropical Pacific Sea Surface Temperature Trends Significant Relative to Internal Variability? *Geophys. Res. Lett.* **44**, 9928–9937 (2017).
24. Ma, J. & Xie, S.-P. Regional Patterns of Sea Surface Temperature Change: A Source of Uncertainty in Future Projections of Precipitation and Atmospheric Circulation. *J. Clim.* **26**, 2482–2501 (2013).
25. Ma, J. & Yu, J.-Y. Linking Centennial Surface Warming Patterns in the Equatorial Pacific to the Relative Strengths of the Walker and Hadley Circulations. *J. Atmos. Sci.* **71**, 3454–3464 (2014).
26. Watanabe, M., Dufresne, J.-L., Kosaka, Y., Mauritsen, T. & Tatebe, H. Enhanced warming constrained by past trends in equatorial Pacific sea surface temperature gradient. *Nat. Clim. Change* **11**, 33–37 (2021).
27. Seager, R. et al. Strengthening tropical Pacific zonal sea surface temperature gradient consistent with rising greenhouse gases. *Nat. Clim. Change* **9**, 517–522 (2019).
28. Huang, P. & Ying, J. A Multimodel Ensemble Pattern Regression Method to Correct the Tropical Pacific SST Change Patterns under Global Warming. *J. Clim.* **28**, 4706–4723 (2015).
29. Ying, J. & Huang, P. Cloud-Radiation Feedback as a Leading Source of Uncertainty in the Tropical Pacific SST Warming Pattern in CMIP5 Models. *J. Clim.* **29**, 3867–3881 (2016a).
30. Ying, J. & Huang, P. The Large-Scale Ocean Dynamical Effect on Uncertainty in the Tropical Pacific SST Warming Pattern in CMIP5 Models. *J. Clim.* **29**, 8051–8065 (2016b).
31. Woodruff, S. D., Slutz, R. J., Jenne, R. L. & Steurer, P. M. A Comprehensive Ocean-Atmosphere Data Set. *Bull. Am. Meteorological Soc.* **68**, 1239–1250 (1987).
32. Parker, D. E. et al. *Natural Climate Variability on Decade-to-Century Time Scales*. (The National Academies Press, 1995).
33. Kaplan, A. et al. Analyses of global sea surface temperature 1856–1991. *J. Geophys. Res.: Oceans* **103**, 18567–18589 (1998).
34. Cane, M. A. et al. Twentieth-Century Sea Surface Temperature Trends. *Science* **275**, 957–960 (1997).
35. Cane, M. A. The evolution of El Niño, past and future. *Earth Planet. Sci. Lett.* **230**, 227–240 (2005).
36. L'Heureux, M. L., Tippett, M. K. & Wang, W. Prediction Challenges From Errors in Tropical Pacific Sea Surface Temperature Trends. *Front. Clim.* **4**, 837483 (2022).
37. Karnauskas, K. B., Seager, R., Kaplan, A., Kushnir, Y. & Cane, M. A. Observed Strengthening of the Zonal Sea Surface Temperature Gradient across the Equatorial Pacific Ocean. *J. Clim.* **22**, 4316–4321 (2009).
38. Allan, R. & Ansell, T. A New Globally Complete Monthly Historical Gridded Mean Sea Level Pressure Dataset (HadSLP2): 1850?2004. *J. Clim.* **19**, 5816–5842 (2006).
39. Kaplan, A., Kushnir, Y. & Cane, M. A. Reduced Space Optimal Interpolation of Historical Marine Sea Level Pressure: 1854?1992. *J. Clim.* **13**, 2987–3002 (2000).
40. Smith, T. M. & Reynolds, R. W. Reconstruction of Monthly Mean Oceanic Sea Level Pressure Based on COADS and Station Data (1854–1997). *J. Atmos. Ocean. Technol.* **21**, 1272–1282 (2004).
41. Sohn, B. J. & Park, S.-C. Strengthened tropical circulations in past three decades inferred from water vapor transport. *J. Geophys. Res.* **115**, D15112 (2010).
42. Zahn, M. & Allan, R. P. Changes in water vapor transports of the ascending branch of the tropical circulation. *Journal of Geophys Res: Atmos* **116**, 16206 (2011).
43. Zhou, Y. P., Xu, K.-M., Sud, Y. C. & Betts, A. K. Recent trends of the tropical hydrological cycle inferred from Global Precipitation Climatology Project and International Satellite Cloud Climatology Project data. *J. Geophys Res: Atmos* **116**, 15197 (2011).
44. Sohn, B. J. et al. Observational evidences of Walker circulation change over the last 30 years contrasting with GCM results. *Clim. Dyn.* **40**, 1721–1732 (2013).
45. Merrifield, M. A. A Shift in Western Tropical Pacific Sea Level Trends during the 1990s. *J. Clim.* **24**, 4126–4138 (2011).
46. Allan, R. P. & Slingo, A. Can current climate model forcings explain the spatial and temporal signatures of decadal OLR variations? *Geophys. Res. Lett.* **29**, 45-41–45-44 (2002).
47. Johnson, N. C., L'Heureux, M. L., Chang, C.-H. & Hu, Z.-Z. On the Delayed Coupling Between Ocean and Atmosphere in Recent Weak El Niño Episodes. *Geophys. Res. Lett.* **46**, 11416–11425 (2019).
48. Ma, S. & Zhou, T. Robust Strengthening and Westward Shift of the Tropical Pacific Walker Circulation during 1979?2012: A Comparison of 7 Sets of Reanalysis Data and 26 CMIP5 Models. *J. Clim.* **29**, 3097–3118 (2016).
49. Henley, B. J. Pacific decadal climate variability: Indices, patterns and tropical-extratropical interactions. *Glob. Planet. Change* **155**, 42–55 (2017).
50. Chen, X. & Wallace, J. M. ENSO-Like Variability: 1900–2013. *J. Clim.* **28**, 9623–9641 (2015).
51. Collins, M. El Niño- or La Niña-like climate change? *Clim. Dyn.* **24**, 89–104 (2005).
52. Held, I. M. et al. Probing the Fast and Slow Components of Global Warming by Returning Abruptly to Preindustrial Forcing. *J. Clim.* **23**, 2418–2427 (2010).
53. Heede, U. K., Fedorov, A. V. & Burls, N. J. Time Scales and Mechanisms for the Tropical Pacific Response to Global Warming: A Tug of War between the Ocean Thermostat and Weaker Walker. *J. Clim.* **33**, 6101–6118 (2020).
54. An, S.-I., Kim, J.-W., Im, S.-H., Kim, B.-M. & Park, J.-H. Recent and future sea surface temperature trends in tropical Pacific warm pool and cold tongue regions. *Clim. Dyn.* **39**, 1373–1383 (2012).
55. Zhang, Y., Wallace, J. M. & Battisti, D. S. ENSO-Like Interdecadal Variability: 1900–93. *J. Clim.* **10**, 1004–1020 (1997).
56. Deser, C., Phillips, A. S. & Hurrell, J. W. Pacific Interdecadal Climate Variability: Linkages between the Tropics and the North Pacific during Boreal Winter since 1900. *J. Clim.* **17**, 3109–3124 (2004).
57. Chen, X. & Wallace, J. M. ENSO-Like Variability: 1900–2013. *J. Clim.* **28**, 9623–9641 (2015).
58. Shin, S. I. & Sardeshmukh, P. D. Critical influence of the pattern of tropical ocean warming on remote climate trends. *Clim. Dyn.* **36**, 1577–1591 (2011).
59. Olonscheck, D., Rugenstein, M. & Marotzke, J. Broad Consistency Between Observed and Simulated Trends in Sea Surface Temperature Patterns. *Geophys. Res. Lett.* **47**, e2019GL086773 (2020).
60. Cane, M. A. In *Using Science Against Famine: Food Security, Famine Early Warning, and El Niño* (ed Glantz, Michael H.) 1363–2914 (University of Bradford, 1997).
61. Bordbar, M. H., Martin, T., Latif, M. & Park, W. Role of internal variability in recent decadal to multidecadal tropical Pacific climate changes. *Geophys. Res. Lett.* **44**, 4246–4255 (2017).
62. Chung, E.-S. et al. Reconciling opposing Walker circulation trends in observations and model projections. *Nat. Clim. Change* **9**, 405–412 (2019).
63. Li, Y. et al. Long-Term Trend of the Tropical Pacific Trade Winds Under Global Warming and Its Causes. *J. Geophys. Res.: Oceans* **124**, 2626–2640 (2019).

64. Kociuba, G. & Power, S. B. Inability of CMIP5 Models to Simulate Recent Strengthening of the Walker Circulation: Implications for Projections. *J. Clim.* **28**, 20–35 (2015).
65. Merlis, T. M. & Schneider, T. Changes in Zonal Surface Temperature Gradients and Walker Circulations in a Wide Range of Climates. *J. Clim.* **24**, 4757–4768 (2011).
66. Yeh, S.-W., Song, S.-Y., Allan, R. P., An, S.-I. & Shin, J. Contrasting response of hydrological cycle over land and ocean to a changing CO<sub>2</sub> pathway. *npj Clim. Atmos. Sci.* **4**, 53 (2021).
67. Wills, R. C., Levine, X. J. & Schneider, T. Local Energetic Constraints on Walker Circulation Strength. *J. Atmos. Sci.* **74**, 1907–1922 (2017).
68. Neelin, J. D. & Held, I. M. Modeling Tropical Convergence Based on the Moist Static Energy Budget. *Monthly Weather Rev.* **115**, 3–12 (1987).
69. Raymond, D. J., Sessions, S. L. & Fuchs, Ž. A theory for the spinup of tropical depressions. *Q. J. R. Meteorological Soc.* **133**, 1743–1754 (2007).
70. Raymond, D. J., Sessions, S. L., Sobel, A. H. & Fuchs, Ž. The Mechanics of Gross Moist Stability. *J. Adv. Model. Earth Syst.* **1**, <https://doi.org/10.3894/JAMES.2009.1.9> (2009).
71. Chou, C. & Chen, C.-A. Depth of Convection and the Weakening of Tropical Circulation in Global Warming. *J. Clim.* **23**, 3019–3030 (2010).
72. Chou, C., Wu, T.-C. & Tan, P.-H. Changes in gross moist stability in the tropics under global warming. *Clim. Dyn.* **41**, 2481–2496 (2013).
73. Betts, A. K. Climate-convection feedbacks: Some further issues. *Clim. Change* **39**, 35–38 (1998).
74. Sandeep, S., Stordal, F., Sardeshmukh, P. D. & Compo, G. P. Pacific Walker Circulation variability in coupled and uncoupled climate models. *Clim. Dyn.* **43**, 103–117 (2014).
75. Clement, A. C., Seager, R., Cane, M. A. & Zebiak, S. E. An Ocean Dynamical Thermostat. *J. Clim.* **9**, 2190–2196 (1996).
76. Ramanathan, V. & Collins, W. Thermodynamic regulation of ocean warming by cirrus clouds deduced from observations of the 1987 El Niño. *Nature* **351**, 27–32 (1991).
77. Hartmann, D. L. & Michelsen, M. L. Large-Scale Effects on the Regulation of Tropical Sea Surface Temperature. *J. Clim.* **6**, 2049–2062 (1993).
78. Pierrehumbert, R. T. Thermostats, Radiator Fins, and the Local Runaway Greenhouse. *J. Atmos. Sci.* **52**, 1784–1806 (1995).
79. Zebiak, S. E. & Cane, M. A. A Model El Niño–Southern Oscillation. *Monthly Weather Rev.* **115**, 2262–2278 (1987).
80. Peters, M. E. & Bretherton, C. S. A Simplified Model of the Walker Circulation with an Interactive Ocean Mixed Layer and Cloud–Radiative Feedbacks. *J. Clim.* **18**, 4216–4234 (2005).
81. Chou, C. & Neelin, J. D. Mechanisms of Global Warming Impacts on Regional Tropical Precipitation. *J. Clim.* **17**, 2688–2701 (2004).
82. Lindzen, R. S., Chou, M.-D. & Hou, A. Y. Does the Earth Have an Adaptive Infrared Iris? *Bull. Am. Meteorological Soc.* **82**, 417–432 (2001).
83. Lee, J., Yang, P., Dessler, A. E., Gao, B.-C. & Platnick, S. Distribution and Radiative Forcing of Tropical Thin Cirrus Clouds. *J. Atmos. Sci.* **66**, 3721–3731 (2009).
84. Hartmann, D. L. & Michelsen, M. L. NO EVIDENCE FOR IRIS. *Bull. Am. Meteorological Soc.* **83**, 249–254 (2002).
85. Fu, Q., Baker, M. & Hartmann, D. L. Tropical cirrus and water vapor: an effective Earth infrared iris feedback? *Atmos. Chem. Phys.* **2**, 31–37 (2002).
86. Lin, B., Wielicki, B. A., Chambers, L. H., Hu, Y. & Xu, K.-M. The Iris Hypothesis: A Negative or Positive Cloud Feedback? *J. Clim.* **15**, 3–7 (2002).
87. Su, H. et al. Variations of tropical upper tropospheric clouds with sea surface temperature and implications for radiative effects. *J. Geophys. Res.: Atmos.* **113**, 9624 (2008).
88. Rondanelli, R. & Lindzen, R. S. Observed variations in convective precipitation fraction and stratiform area with sea surface temperature. *J. Geophys. Res.: Atmos.* **113**, 10064 (2008).
89. Choi, Y.-S. et al. Revisiting the iris effect of tropical cirrus clouds with TRMM and A-Train satellite data. *J. Geophys. Res.: Atmospheres* **122**, 5917–5931 (2017).
90. Mauritsen, T. & Stevens, B. Missing iris effect as a possible cause of muted hydrological change and high climate sensitivity in models. *Nat. Geosci.* **8**, 346–351 (2015).
91. Lee, S. A theory for polar amplification from a general circulation perspective. *Asia-Pac. J. Atmos. Sci.* **50**, 31–43 (2014).
92. Charney, J. G. & Drazin, P. G. Propagation of planetary-scale disturbances from the lower into the upper atmosphere. *J. Geophys. Res. (1896-1977)* **66**, 83–109 (1961).
93. Lee, S., Gong, T., Johnson, N., Feldstein, S. B. & Pollard, D. On the Possible Link between Tropical Convection and the Northern Hemisphere Arctic Surface Air Temperature Change between 1958 and 2001. *J. Clim.* **24**, 4350–4367 (2011).
94. Yoo, C., Feldstein, S. & Lee, S. The impact of the Madden-Julian Oscillation trend on the Arctic amplification of surface air temperature during the 1979–2008 boreal winter. *Geophys. Res. Lett.* **38**, L049881 (2011).
95. Baggett, C. & Lee, S. Arctic Warming Induced by Tropically Forced Tapping of Available Potential Energy and the Role of the Planetary-Scale Waves. *J. Atmos. Sci.* **72**, 1562–1568 (2015).
96. Lee, S., Feldstein, S., Pollard, D. & White, T. Do Planetary Wave Dynamics Contribute to Equable Climates? *J. Clim.* **24**, 2391–2404 (2011).
97. Lea, D. W., Pak, D. K. & Spero, H. J. Climate Impact of Late Quaternary Equatorial Pacific Sea Surface Temperature Variations. *Science* **289**, 1719–1724 (2000).
98. Tierney, J. E., Haywood, A. M., Feng, R., Bhattacharya, T. & Otto-Bliesner, B. L. Pliocene Warmth Consistent With Greenhouse Gas Forcing. *Geophys. Res. Lett.* **46**, 9136–9144 (2019).
99. Wara, M. W., Ravelo, A. C. & Delaney, M. L. Permanent El Niño-Like Conditions During the Pliocene Warm Period. *Science* **309**, 758–761 (2005).
100. Gulev, S. K. et al. In Climate Change 2021: The Physical Science Basis. *Contribution of Working Group I to the Sixth Assessment Report of the Intergovernmental Panel on Climate Change* Vol. Contribution of Working Group I to the Sixth Assessment Report of the Intergovernmental Panel on Climate Change (eds Masson-Delmotte, V. et al.) Ch. 2, 287–422 (Cambridge University Press, 2021).
101. Koutavas, A., Lynch-Stieglitz, J., Marchitto, T. M. & Sachs, J. P. El Niño-Like Pattern in Ice Age Tropical Pacific Sea Surface Temperature. *Science* **297**, 226–230 (2002).
102. Stott, L., Poulsen, C., Lund, S. & Thunell, R. Super ENSO and Global Climate Oscillations at Millennial Time Scales. *Science* **297**, 222–226 (2002).
103. Visser, K., Thunell, R. & Stott, L. Magnitude and timing of temperature change in the Indo-Pacific warm pool during deglaciation. *Nature* **421**, 152–155 (2003).
104. Zhang, Y. G., Pagani, M. & Liu, Z. A 12-Million-Year Temperature History of the Tropical Pacific Ocean. *Science* **344**, 84–87 (2014).
105. Lea, D. W. Not So Permanent El Niño. *Science* **344**, 52–53 (2014).
106. Lindzen, R. S. & Nigam, S. On the Role of Sea Surface Temperature Gradients in Forcing Low-Level Winds and Convergence in the Tropics. *J. Atmos. Sci.* **44**, 2418–2436 (1987).
107. Back, L. E. & Bretherton, C. S. On the Relationship between SST Gradients, Boundary Layer Winds, and Convergence over the Tropical Oceans. *J. Clim.* **22**, 4182–4196 (2009).
108. Duffy, M. L., O’Gorman, P. A. & Back, L. E. Importance of Laplacian of Low-Level Warming for the Response of Precipitation to Climate Change over Tropical Oceans. *J. Clim.* **33**, 4403–4417 (2020).
109. Seager, R. et al. Adjustment of the atmospheric circulation to tropical Pacific SST anomalies: Variability of transient eddy propagation in the Pacific–North America sector. *Q. J. R. Meteorological Soc.* **136**, 277–296 (2010).
110. Johnson, N. C. & Xie, S.-P. Changes in the sea surface temperature threshold for tropical convection. *Nat. Geosci.* **3**, 842–845 (2010).
111. Izumo, T., Vialard, J., Lengaigne, M. & Suresh, I. Relevance of Relative Sea Surface Temperature for Tropical Rainfall Interannual Variability. *Geophys. Res. Lett.* **47**, e2019GL086182 (2020).
112. Capotondi, A. et al. Understanding ENSO Diversity. *Bull. Am. Meteorological Soc.* **96**, 921–938 (2015).
113. L’Heureux, M. L. et al. Observing and Predicting the 2015/16 El Niño. *Bull. Am. Meteorological Soc.* **98**, 1363–1382 (2017).
114. Newman, M., Wittenberg, A. T., Cheng, L., Compo, G. P. & Smith, C. A. The Extreme 2015/16 El Niño, in the Context of Historical Climate Variability and Change. *Bull. Am. Meteorological Soc.* **99**, S16–S20 (2018).
115. Lee, S.-K. et al. On the Fragile Relationship Between El Niño and California Rainfall. *Geophys. Res. Lett.* **45**, 907–915 (2018).
116. He, J. et al. Precipitation Sensitivity to Local Variations in Tropical Sea Surface Temperature. *J. Clim.* **31**, 9225–9238 (2018).
117. Chiodi, A. M. & Harrison, D. E. Global Seasonal Precipitation Anomalies Robustly Associated with El Niño and La Niña Events? An OLR Perspective. *J. Clim.* **28**, 6133–6159 (2015).
118. Johnson, N. C. & Kosaka, Y. The impact of eastern equatorial Pacific convection on the diversity of boreal winter El Niño teleconnection patterns. *Clim. Dyn.* **47**, 3737–3765 (2016).
119. L’Heureux, M. L. et al. In *El Niño Southern Oscillation in a Changing Climate* 227–246 (2020).
120. Nicholls, N. Recent trends in the seasonal and temporal behaviour of the El Niño–Southern Oscillation. *Geophys. Res. Lett.* **35**, L034499 (2008).
121. Stein, K., Timmermann, A., Schneider, N., Jin, F.-F. & Stuecker, M. F. ENSO Seasonal Synchronization Theory. *J. Clim.* **27**, 5285–5310 (2014).
122. Krishnamurthy, L. et al. The Seasonality of the Great Plains Low-Level Jet and ENSO Relationship. *J. Clim.* **28**, 4525–4544 (2015).
123. Lee, S.-K. et al. US regional tornado outbreaks and their links to spring ENSO phases and North Atlantic SST variability. *Environ. Res. Lett.* **11**, 044008 (2016).
124. Anderson, W., Seager, R., Baethgen, W. & Cane, M. Life cycles of agriculturally relevant ENSO teleconnections in North and South America. *Int. J. Climatol.* **37**, 3297–3318 (2017).

125. Zhang, W. et al. Unraveling El Niño's impact on the East Asian Monsoon and Yangtze River summer flooding. *Geophys. Res. Lett.* **43**, 11,375–311,382 (2016).
126. Goddard, L. & Gershunov, A. In *El Niño Southern Oscillation in a Changing Climate* 361–375 (2020).
127. Vecchi, G. A. & Soden, B. J. Effect of remote sea surface temperature change on tropical cyclone potential intensity. *Nature* **450**, 1066–1070 (2007).
128. Ramsay, H. A. & Sobel, A. H. Effects of Relative and Absolute Sea Surface Temperature on Tropical Cyclone Potential Intensity Using a Single-Column Model. *J. Clim.* **24**, 183–193 (2011).
129. Taschetto, A. S. et al. In *El Niño Southern Oscillation in a Changing Climate* 309–335 (2020).
130. Kosaka, Y. & Xie, S.-P. Recent global-warming hiatus tied to equatorial Pacific surface cooling. *Nature* **501**, 403–407 (2013).
131. Delworth, T. L., Zeng, F., Rosati, A., Vecchi, G. A. & Wittenberg, A. T. A Link between the Hiatus in Global Warming and North American Drought. *J. Clim.* **28**, 3834–3845 (2015).
132. Lyon, B. Seasonal Drought in the Greater Horn of Africa and Its Recent Increase during the March–May Long Rains. *J. Clim.* **27**, 7953–7975 (2014).
133. Yang, W., Seager, R., Cane, M. A. & Lyon, B. The East African Long Rains in Observations and Models. *J. Clim.* **27**, 7185–7202 (2014).
134. McGregor, G. R. & Ebi, K. El Niño Southern Oscillation (ENSO) and Health: An Overview for Climate and Health Researchers. *Atmosphere* **9**, 282 (2018).
135. Anyamba, A. et al. Global Disease Outbreaks Associated with the 2015–2016 El Niño Event. *Sci. Rep.* **9**, 1930 (2019).
136. Church, J. A. et al. In *Climate Change 2013: The Physical Science Basis. Contribution of Working Group I to the Fifth Assessment Report of the Intergovernmental Panel on Climate Change* (ed Stocker, T. F. et al.) (Cambridge University, 2013).
137. Eddebbar, Y. A. et al. Impacts of ENSO on air-sea oxygen exchange: Observations and mechanisms. *Glob. Biogeochemical Cycles* **31**, 901–921 (2017).
138. Adeel, Z. & Glantz, M. H. El Niño of the century: once burnt, twice shy? *Glob. Environ. Change* **11**, 171–174 (2001).
139. Sponberg, K. In *Compendium of Climatological Impacts Vol. 1* 13 pp. (University Corporation for Atmospheric Research, National Oceanic and Atmospheric Administration, Office of Global Programs, 1999).
140. McKinley, G. A., Fay, A. R., Lovenduski, N. S. & Pilcher, D. J. Natural Variability and Anthropogenic Trends in the Ocean Carbon Sink. *Annu. Rev. Mar. Sci.* **9**, 125–150 (2017).
141. Betts, R. A. et al. In *El Niño Southern Oscillation in a Changing Climate* 453–470 (2020).
142. Chen, C., Cane, M. A., Wittenberg, A. T. & Chen, D. ENSO in the CMIP5 Simulations: Life Cycles, Diversity, and Responses to Climate Change. *J. Clim.* **30**, 775–801 (2017).
143. Graham, F. S., Wittenberg, A. T., Brown, J. N., Marsland, S. J. & Holbrook, N. J. Understanding the double peaked El Niño in coupled GCMs. *Clim. Dyn.* **48**, 2045–2063 (2017).
144. Guilyardi, E., Capotondi, A., Lengaigne, M., Thual, S. & Wittenberg, A. T. In *El Niño Southern Oscillation in a Changing Climate* 199–226 (2020).
145. Fedorov, A. V., Hu, S., Wittenberg, A. T., Levine, A. F. Z. & Deser, C. In *El Niño Southern Oscillation in a Changing Climate* 173–198 (2020).
146. Ding, H., Newman, M., Alexander, M. A. & Wittenberg, A. T. Relating CMIP5 Model Biases to Seasonal Forecast Skill in the Tropical Pacific. *Geophys. Res. Lett.* **47**, e2019GL086765 (2020).
147. Huang, P. & Chen, D. Enlarged Asymmetry of Tropical Pacific Rainfall Anomalies Induced by El Niño and La Niña under Global Warming. *J. Clim.* **30**, 1327–1343 (2017).
148. Lopez, H., Lee, S.-K., Kim, D., Wittenberg, A. T. & Yeh, S.-W. Projections of faster onset and slower decay of El Niño in the 21st century. *Nat. Commun.* **13**, 1915 (2022).
149. Dommenges, D. & Vijayeta, A. Simulated future changes in ENSO dynamics in the framework of the linear recharge oscillator model. *Clim. Dyn.* **53**, 4233–4248 (2019).
150. Wang, B. et al. Historical change of El Niño properties sheds light on future changes of extreme El Niño. *Proc. Natl Acad. Sci.* **116**, 22512–22517 (2019).
151. Wengel, C. et al. Future high-resolution El Niño/Southern Oscillation dynamics. *Nat. Clim. Change* **11**, 758–765 (2021).
152. DiNezio, P. N. et al. Mean Climate Controls on the Simulated Response of ENSO to Increasing Greenhouse Gases. *J. Clim.* **25**, 7399–7420 (2012).
153. Huang, P. & Xie, S.-P. Mechanisms of change in ENSO-induced tropical Pacific rainfall variability in a warming climate. *Nat. Geosci.* **8**, 922–926 (2015).
154. Huang, P. Time-Varying Response of ENSO-Induced Tropical Pacific Rainfall to Global Warming in CMIP5 Models. Part II: Intermodel Uncertainty. *J. Clim.* **30**, 595–608 (2017).
155. Stevenson, S., Wittenberg, A. T., Fasullo, J., Coats, S. & Otto-Bliesner, B. Understanding Diverse Model Projections of Future Extreme El Niño. *J. Clim.* **34**, 449–464 (2021).
156. Bellenger, H., Guilyardi, E., Leloup, J., Lengaigne, M. & Vialard, J. ENSO representation in climate models: from CMIP3 to CMIP5. *Clim. Dyn.* **42**, 1999–2018 (2014).
157. Vijayeta, A. & Dommenges, D. An evaluation of ENSO dynamics in CMIP simulations in the framework of the recharge oscillator model. *Clim. Dyn.* **51**, 1753–1771 (2018).
158. Planton, Y. Y. et al. Evaluating Climate Models with the CLIVAR 2020 ENSO Metrics Package. *Bull. Am. Meteorological Soc.* **102**, E193–E217 (2021).
159. Chen, H.-C., Fei-Fei-Jin, Zhao, S., Wittenberg, A. T. & Xie, S. ENSO Dynamics in the E3SM-1-0, CESM2, and GFDL-CM4 Climate Models. *J. Clim.* **34**, 9365–9384 (2021).
160. Dong, Y. et al. Intermodel Spread in the Pattern Effect and Its Contribution to Climate Sensitivity in CMIP5 and CMIP6 Models. *J. Clim.* **33**, 7755–7775 (2020).
161. Andrews, T. et al. Accounting for Changing Temperature Patterns Increases Historical Estimates of Climate Sensitivity. *Geophys. Res. Lett.* **45**, 8490–8499 (2018).
162. Zhou, C., Zelinka, M. D. & Klein, S. A. Impact of decadal cloud variations on the Earth's energy budget. *Nat. Geosci.* **9**, 871–874 (2016).
163. Webb, M. J. et al. The Cloud Feedback Model Intercomparison Project (CFMIP) contribution to CMIP6. *Geosci. Model Dev.* **10**, 359–384 (2017).
164. Andrews, T. & Webb, M. J. The Dependence of Global Cloud and Lapse Rate Feedbacks on the Spatial Structure of Tropical Pacific Warming. *J. Clim.* **31**, 641–654 (2018).
165. Rugenstein, M. et al. Equilibrium Climate Sensitivity Estimated by Equilibrating Climate Models. *Geophys. Res. Lett.* **47**, e2019GL083898 (2020).
166. Yeh, S.-W. et al. ENSO Atmospheric Teleconnections and Their Response to Greenhouse Gas Forcing. *Rev. Geophysics* **56**, 185–206 (2018).
167. Sprintall, J., Cravatte, S., Dewitte, B., Du, Y. & Gupta, A. S. In *El Niño Southern Oscillation in a Changing Climate* 337–359 (2020).
168. Beverley, J. D., Collins, M., Lambert, F. H. & Chadwick, R. Future Changes to El Niño Teleconnections over the North Pacific and North America. *J. Clim.* **34**, 6191–6205 (2021).
169. Yun, K.-S. et al. Increasing ENSO–rainfall variability due to changes in future tropical temperature–rainfall relationship. *Commun. Earth Environ.* **2**, 43 (2021).
170. Yang, Y.-M., Park, J.-H., An, S.-I., Wang, B. & Luo, X. Mean sea surface temperature changes influence ENSO-related precipitation changes in the mid-latitudes. *Nat. Commun.* **12**, 1495 (2021).
171. Cai, W. et al. Pantropical climate interactions. *Science* **363**, eaav4236 (2019).
172. Li, C., Dommenges, D. & McGregor, S. Trans-basin Atlantic-Pacific connections further weakened by common model Pacific mean SST biases. *Nat. Commun.* **11**, 5677 (2020).
173. Maloney, E. D., Adames, Á. F. & Bui, H. X. Madden-Julian oscillation changes under anthropogenic warming. *Nat. Clim. Change* **9**, 26–33 (2019).
174. Jiang, X. et al. Fifty Years of Research on the Madden-Julian Oscillation: Recent Progress, Challenges, and Perspectives. *J. Geophys. Res.: Atmospheres* **125**, e2019JD030911 (2020).
175. Lin, I.-I. et al. In *El Niño Southern Oscillation in a Changing Climate* 377–408 (2020).
176. Cravatte, S. et al. First Report of TPOS 2020. *GOOS-215*, 200 pp. (2016).
177. Kessler, W. S. et al. TPOS 2020 Final Report. (2021).
178. Knutson, T. R., Zeng, F. & Wittenberg, A. T. Multimodel assessment of extreme annual-mean warm anomalies during 2013 over regions of Australia and the western tropical Pacific. Section 8 of "Explaining extreme events of 2013 from a climate perspective." *Bull. Am. Meteorol. Soc.* **95**, Si-Siv, S1-S97 (2014).
179. Tippett, M. K., L'Heureux, M. L., Becker, E. J. & Kumar, A. Excessive Momentum and False Alarms in Late-Spring ENSO Forecasts. *Geophys. Res. Lett.* **47**, e2020GL087008 (2020).
180. Shin, C.-S. & Huang, B. A spurious warming trend in the NMME equatorial Pacific SST hindcasts. *Clim. Dyn.* **53**, 7287–7303 (2019).
181. Sherwood, S. C. & Nishant, N. Atmospheric changes through 2012 as shown by iteratively homogenized radiosonde temperature and wind data (IUKv2). *Environ. Res. Lett.* **10**, 054007 (2015).
182. Po-Chedley, S. & Fu, Q. Discrepancies in tropical upper tropospheric warming between atmospheric circulation models and satellites. *Environ. Res. Lett.* **7**, 044018 (2012).
183. Sohn, B.-J., Lee, S., Chung, E.-S. & Song, H.-J. The Role of the Dry Static Stability for the Recent Change in the Pacific Walker Circulation. *J. Clim.* **29**, 2765–2779 (2016).
184. Po-Chedley, S. et al. Natural variability contributes to model–satellite differences in tropical tropospheric warming. *Proc. Natl Acad. Sci.* **118**, e2020962118 (2021).
185. Duffy, M. L. & O'Gorman, P. A. An energetic evaluation of the response of the Walker circulation to warming. *Earth and Space Science Open Archive*, 25, <https://doi.org/10.1002/essoar.10511736.1>.

186. Mapes, B. & Neale, R. Parameterizing Convective Organization to Escape the Entrainment Dilemma. *J. Adv. Model. Earth Syst.* **3**, 42 (2011).
187. Satoh, M. et al. Global Cloud-Resolving Models. *Curr. Clim. Change Rep.* **5**, 172–184 (2019).
188. Brenowitz, N. D. & Bretherton, C. S. Prognostic Validation of a Neural Network Unified Physics Parameterization. *Geophys. Res. Lett.* **45**, 6289–6298 (2018).
189. O’Gorman, P. A. & Dwyer, J. G. Using Machine Learning to Parameterize Moist Convection: Potential for Modeling of Climate, Climate Change, and Extreme Events. *J. Adv. Modeling Earth Syst.* **10**, 2548–2563 (2018).
190. Rasp, S., Pritchard, M. S. & Gentine, P. Deep learning to represent subgrid processes in climate models. *Proc. Natl. Acad. Sci.* **115**, 9684–9689, (2018).
191. Dong, Y., Armour, K. C., Battisti, D. S. & Blanchard-Wrigglesworth, E. Two-way teleconnections between the Southern Ocean and the tropical Pacific via a dynamic feedback. *J. Clim.* **35**, 1–37, (2022).
192. Liu, B. et al. Will Increasing Climate Model Resolution Be Beneficial for ENSO Simulation? *Geophys. Res. Lett.* **49**, e2021GL096932 (2022).
193. Christensen, H. M. & Berner, J. From reliable weather forecasts to skilful climate response: A dynamical systems approach. *Q. J. R. Meteorological Soc.* **145**, 1052–1069 (2019).
194. Ma, H.-Y. et al. On the Correspondence between Mean Forecast Errors and Climate Errors in CMIP5 Models. *J. Clim.* **27**, 1781–1798 (2014).
195. Pegion, K. et al. The Subseasonal Experiment (SubX): A Multimodel Subseasonal Prediction Experiment. *Bull. Am. Meteorological Soc.* **100**, 2043–2060 (2019).
196. Becker, E. J., Kirtman, B. P., L’Heureux, M., Muñoz, Á. G. & Pegion, K. A Decade of the North American Multimodel Ensemble (NMME): Research, Application, and Future Directions. *Bull. Am. Meteorological Soc.* **103**, E973–E995 (2022).
197. Shepherd, T. G. Storyline approach to the construction of regional climate change information. Proceedings of the Royal Society A. *Math., Phys. Eng. Sci.* **475**, 20190013 (2019).
198. Shepherd, T. G. & Sobel, A. H. Localness in Climate Change. *Comp. Stud. South Asia, Afr. Middle East* **40**, 7–16 (2020).
199. Solomon, A. & Newman, M. Reconciling disparate twentieth-century Indo-Pacific ocean temperature trends in the instrumental record. *Nat. Clim. Change* **2**, 691–699 (2012).
200. Sardeshmukh, P. D. & Hoskins, B. J. The Generation of Global Rotational Flow by Steady Idealized Tropical Divergence. *J. Atmos. Sci.* **45**, 1228–1251 (1988).

## ACKNOWLEDGEMENTS

S.L. was supported by National Science Foundation Grant AGS-1948667. PAO’G was supported by NSF AGS 1749986. R.S. was supported by NSF AGS 21-01214 and 19-34363 and NOAA NA20OAR4310379. Figures 5 and 6 were created by climate.gov.

Comments by two anonymous reviewers and Arun Kumar, who served as an internal reviewer, led to improvement of this manuscript.

## AUTHOR CONTRIBUTIONS

S.L. and M.L. initiated this effort. M.L., S.L., and A.T.W. led the second, third, and fourth sections, respectively. All authors collated and wrote the manuscript. In particular, R.S. made substantial contributions to the second, third, and sixth sections. P.A.O’G. made substantial contributions to the third and fifth sections. N.C.J. made substantial contributions to the second and fourth sections.

## COMPETING INTERESTS

The authors declare no competing interests.

## ADDITIONAL INFORMATION

**Correspondence** and requests for materials should be addressed to Sukyoung Lee.

**Reprints and permission information** is available at <http://www.nature.com/reprints>

**Publisher’s note** Springer Nature remains neutral with regard to jurisdictional claims in published maps and institutional affiliations.



**Open Access** This article is licensed under a Creative Commons Attribution 4.0 International License, which permits use, sharing, adaptation, distribution and reproduction in any medium or format, as long as you give appropriate credit to the original author(s) and the source, provide a link to the Creative Commons license, and indicate if changes were made. The images or other third party material in this article are included in the article’s Creative Commons license, unless indicated otherwise in a credit line to the material. If material is not included in the article’s Creative Commons license and your intended use is not permitted by statutory regulation or exceeds the permitted use, you will need to obtain permission directly from the copyright holder. To view a copy of this license, visit <http://creativecommons.org/licenses/by/4.0/>.

© The Author(s) 2022